

First Order Analysis for Automotive Body Structure Design – Part 1 : Overview and Applications

Hidekazu Nishigaki, Tatsuyuki Amago, Hideki Sugiura, Yoshio Kojima
Toyota Central R&D Labs., Inc.

Shinji Nishiwaki
Kyoto University

Noboru Kikuchi
The University of Michigan

Copyright © 2003 SAE International

ABSTRACT

Computer Aided Engineering (CAE) has been successfully utilized in automotive industries. CAE numerically estimates the performance of automobiles and proposes alternative ideas that lead to the higher performance without building prototypes. Most automotive designers, however, cannot directly use CAE due to the sophisticated operations. In order to overcome this problem, we proposed a new concept of CAE, First Order Analysis (FOA). The basic ideas include (1) graphic interfaces using Microsoft/Excel to achieve a product oriented analysis (2) use the knowledge of the mechanics of materials to provide the useful information for designers, and (3) the topology optimization method using beam and panel elements. In this paper, outline of FOA and application are introduced

INTRODUCTION

CAE (Computer Aided Engineering) has been widely accepted in many mechanical industries such as automotive industries since this concept was first proposed by J. Lemon at SDRC in 1980. CAE makes it possible for us to quantitatively estimate the performance of mechanical structures and mechanisms such as a body structure and a suspension system in automobiles using the finite element method and dynamic analysis. However, almost all automotive design engineers, in fact, cannot utilize CAE applications by themselves. This is because specific skills and knowledge are required for the sophisticated operations in CAE, and requires a huge amount of time to construct an analysis model. In order to overcome this problem, we proposed a new concept of CAE, First Order Analysis (FOA) (Nishigaki [6]).

In this paper, the following are introduced : Outline of FOA and the application. First, needs and roles of FOA are briefly discussed. Next, two types of

basic applications based on the concept of FOA are presented. Finally, the specialized applications based on the basic ones are proposed. The availability of its concept is demonstrated by the applications for under body and suspension.

FIRST ORDER ANALYSIS (FOA)

NEEDS AND ROLES OF FOA

The terminology of Computer Aided Engineering (CAE) was introduced by J. Lemon [9] at SDRC in order to define engineering analysis in the computer age, and this concept has been widely accepted in automotive industries. The main objectives of CAE are (1) to numerically estimate the design criteria at the design phase, and (2) to obtain an alternative design if a current design does not satisfy them, without building prototypes.

Recent advances in the structural analysis have played important roles in CAE as the commercial finite element (FE) codes such as MSC/NASTRAN and ABAQUS have been improved and widely used. They can quantitatively estimate the static and dynamic performance of automotive body structures and propose alternative ideas that lead to the higher performance using the structural optimization scheme.

In the actual development of automobiles, however, CAE has been utilized not by the automotive design engineers at the design phase, but by the special CAE engineers who are well-trained and have comprehensive understanding regarding theory and applications of CAE at the evaluation phase. Figure 1 shows a flow diagram of automotive structure development. As shown in this figure, automotive bodies are developed by incorporating of two divisions, the design division and evaluation division. In the design division, first, a few concept designs are selected by

body design engineers and planners. After determining these, the detailed design is also performed by design engineers. In this phase, the 3D CAD system is usually utilized to draw design drafts. Design engineers sometimes need to use their own experience accumulated from previous developments and knowledge of structural mechanics in order to obtain the best choice among drafts. They also must theoretically understand the reasons why this produces the highest performance as an automotive body structure using analytical ways such as a free-body diagram. However, they do not usually use sophisticated numerical methods including FEM.

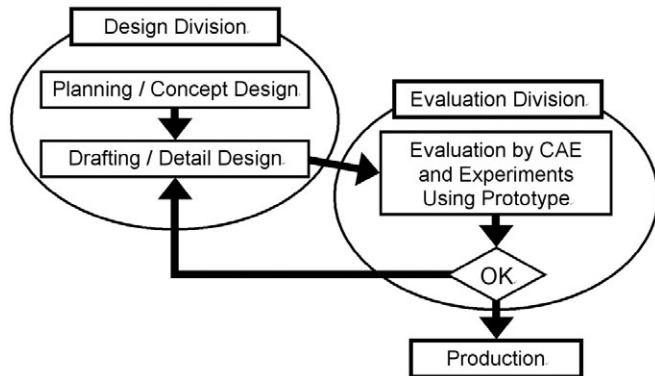


Figure 1. Flow of Automotive structure development.

After the designs are selected, they are given to the evaluation division for performance evaluation using CAE and prototype experiments. In this phase, the main roles are carried out by the special CAE engineers even though design engineers continue to maintain close communications with them. These engineers assign FE modelers the design drafts to build FE models. In general, constructing such a model is very time-consuming. It usually takes about one month to construct a whole vehicle structure. This is also quite a hard and complex task. Especially, setting of boundary conditions and joint modeling are important, and need to be appropriately configured in order to attain the sufficiently accurate results. It is true that accuracy in structural analysis is an important factor to accurately assess the performance. Therefore, CAE engineers must know comprehensive knowledge of numerical analysis and modeling.

After evaluating the performance using postprocessing in this division, design engineers reconsider the configuration of the design draft by discussing with the CAE engineers. The CAE engineers also suggest alternative configurations satisfying all design criteria using the optimization method. However, the final decision of design change is usually made by design engineers with comprehensive information from planning concepts through manufacturing restrictions. Once the design changes occur, the CAE model is reconfigured and the design criteria are re-examined. If

these modifications do not provide sufficient performance, the development flow is iterated.

As mentioned above, no ideal CAE is thoroughly performed by automotive design engineers in reality. That is, the real CAE is being used not as a design tool but as an evaluation tool of a design draft. Therefore, design engineers usually do not have any CAE system to help their decision making besides the CAD system. The reasons why the current CAE system is not accepted by design engineers are summarized as follows:

(1) Commercial software vendors usually recognize that automotive design engineers have enough knowledge of CAE. However, they do not have much knowledge of computer hardware and software since their role is not only structural design but also comprehensive design including the selection of part supplies and the manufacturing process. It is not an exaggeration to say that they have hardly studied applications of solid mechanics and numerical analysis. Therefore, the current CAE system is too complex to use in routine design work. On the other hand, the commercial codes include many options to deal with almost all structural analyses. Much knowledge is required to appropriately select parameters for each analysis. This tendency makes it difficult for design engineers to utilize them, and requires the use of special CAE engineers.

(2) Making analysis models with boundary conditions is complex and very time-consuming even though we use automesh generators. Design engineers cannot spend time for this because they usually need to make a comprehensive decision on a design within a limited development term.

(3) Design engineers always need to study and verify mechanical properties and structural mechanisms related to a selected design draft based on their experience and simple mechanics. However, it is rather hard to understand them using the current CAE models because these models usually have more than 1,000,000 degrees of freedom. Further, the current CAE programs do not provide enough information to study the structural mechanisms. They usually give only the displacement and stress distribution in the static analysis. It is difficult for design engineers to evaluate the design functions only using these physical properties. They need different, but more meaningful physical values.

As we discussed above, one of the most critical problems for the current automotive development using CAE is that the CAE system for the design engineers' use is not established. This situation sometimes causes a lot of iterations of design changes because few design engineers theoretically choose the best design drafts using CAE. This may be a reason why we can not reduce the developing span nor reach real optimal structures in the global sense.

In order to overcome this problem, we propose a new concept of CAE for design engineers, *First Order*

Analysis (FOA). This CAE can solve the problems listed above in the following ways:

(1) Design engineers usually have their own notebook-type computers on their desks. They are accustomed to using Microsoft/Excel. Therefore, all graphic interfaces for design engineers are developed using Excel. Each analysis program is performed with only their own notebook computers, and is specialized for each design part using a template.

(2) The analysis time including model construction must be less than three hours. However, design engineers usually need only the qualitative analysis. The quantitative values are not as important at the design phase. Therefore, automotive body models are constructed using only structural beam and panel elements. The standard templates for modeling are prepared to reduce modeling time. A new model can quickly be made by modifying these templates. Each analysis program and template corresponding to each body part is particularized in order to reduce analysis parameters, but is hierarchically interconnected.

(3) The configuration using beam and panel elements provides many more suggestions regarding mechanical properties than the usual finite elements such as hexagonal and shell elements because these elements may emphasize the effects and characteristics of the elements. Moreover, the programs graphically show the distribution of physical properties such as strain energy in the body structure to help design engineers to easily understand its mechanics.

Thus, body design engineers graphically and quickly understand the qualitative properties of the design drafts, and choose the best idea among them based on FOA at the design phase. However, note that the usual CAE analysis based on FEM has an important role even though FOA is performed by design engineers. This is because only a qualitative evaluation is done by FOA. The quantitative and accurate evaluation of the performance criteria must be performed for the automobile development in the evaluation division. That is, FOA has a mutually complementary relation with the usual CAE. A combination of them provides a possibility of a further integrated CAE.

COMPONENTS OF FOA

The essential issues at the design phase are to evaluate the design criteria with respect to automotive body frames and panels, and to obtain an optimal layout of them and an optimal cross-sectional shape of each frame. The basic ideas of FOA include (1) graphic interfaces for automotive design engineers using Microsoft/Excel (2) use of sophisticated formulations based on the theory of mechanics of materials, (3) the topology optimization method using function oriented elements. FOA considers the following components to accomplish them.

The static and eigen-value analyses using beam and panel elements

The static stiffness is important to evaluate the drivability and strength. Modal frequencies and mode shapes are analyzed to assess the performance of comparatively lower frequency vibration and comfort (Howell and Chang[4]).

A beam component follows formulization of the usual alignment elastic beam (Rao[7]). In addition, it also makes it possible to give the rotation spring of three degrees of freedom to an end in order to express important joint stiffness in vehicles structure.

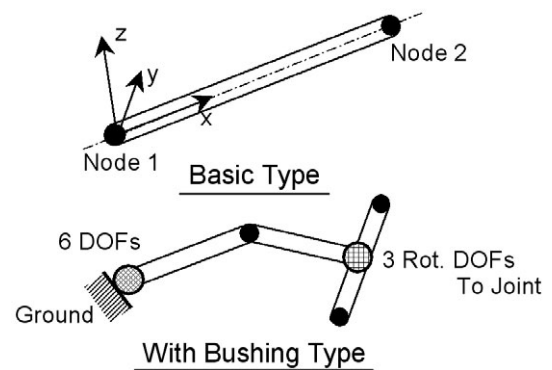
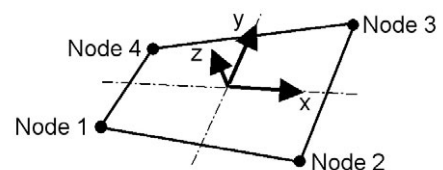


Figure 2. Configuration of beam element

The stress assumed method is used to formulate panel elements. The basic idea is based on the mixed approach. Advantages of this method are that (1) we can assume an independent interpolation function of the stress distribution of the shape function of the displacement, and (2) the accuracy can be maintained even if the shape of the element is distorted or its size is comparatively large. Here, we briefly describe the formulations (See details in Sekiguchi and Kikuchi [15]).



$$Stress \ s = \begin{Bmatrix} \sigma_x \\ \sigma_y \\ \tau \end{Bmatrix} = \begin{Bmatrix} C_{11} + C_{12}y \\ C_{21} + C_{22}x \\ C_{31} \end{Bmatrix}$$

$$Disp. \ u = \begin{Bmatrix} u_x \\ u_y \end{Bmatrix} = \begin{Bmatrix} a_0 + a_1x + a_2y + a_3xy \\ b_0 + b_1x + b_2y + b_3xy \end{Bmatrix}$$

Inconsistency Between Stresses and Displacement Is Relaxed Using Least Square Method.

Figure 3. Configuration of panel element

Topology optimization using beam and panel elements

This optimization method determines the configurations of automotive body frames and the locations of the structural reinforcements by the ground structure approach. This approach using truss elements is not new (see details in Bendsøe [1]). The earliest effort was made by Dorn et al. [3]. In this research, a beam element is treated as a design structure. This is because (1) a beam element has six degrees of freedom, and it provides an optimal solution in all loading cases including a moment loading, (2) it is practical rather than a truss element, and (3) sizing optimization including the cross-sectional design can simultaneously be performed. Note that the cross-sectional shape does not influence the physical properties of a truss element since the truss does not express the bending effect.

The key idea is based on the ground structure approach and the minimization of the mean compliance in order to maximize the global structural stiffness. In the ground structure approach, first, a set of fixed nodal points and all possible connections using beam elements are provided as shown in Figure 4. We seek to find an optimal beam configuration by eliminating unnecessary beams in the design domain using an optimization scheme. Panel and beam elements can be added as the non-design elements to represent the actual configuration of the design part.

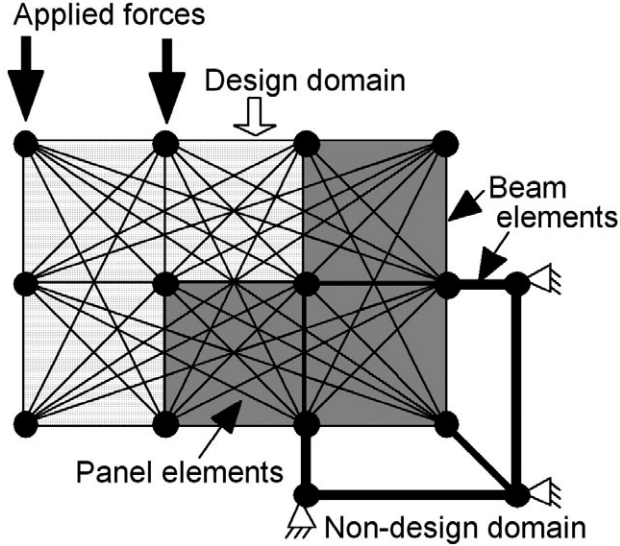


Figure 4. Initial setting of beam and elements

Since the automotive body frame consisted of thin-walled sections, the two types of the sections are prepared: a solid circle section and a thin-walled circle section (Figure 5).

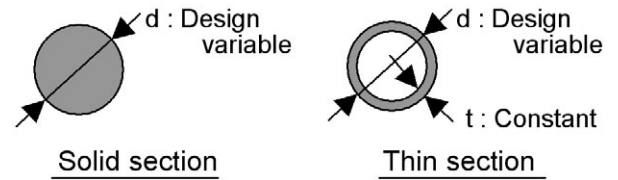


Figure 5. Section type used by topology optimization

Consider that an elastic three-dimensional structure, Ω , is fixed at boundary Γ_d and is subjected to a load representing a force vector f at boundary Γ_t . Body forces applied to the structure are assumed to be ignored for simplicity in the formulation. Let u be the displacement vector due to the applied force. Then, the mean compliance l (Bendsøe and Kikuchi [2]) defined by

$$l = f \cdot u = f^T u \quad (1)$$

is interpreted as the measure of stiffness at boundary Γ_t . That is, by minimizing or decreasing l , we can obtain sufficient stiffness Γ_t . Since the displacement field satisfies the following equilibrium equation:

$$Ku = f \quad (2)$$

where K is the global stiffness matrix, we have

$$l = f^T u = u^T Ku \quad (3)$$

Taking the derivative of Eqn (20), i.e., the sensitivity, with respect to a design variable a , yields,

$$\frac{\partial l}{\partial a} = -u^T \frac{\partial K}{\partial a} u \quad (4)$$

APPLICATION AND EXAMPLES

The application developed based on the view of FOA is classified into two types. One is basic application for arbitrary structures, which is applied to all applications. The other is the product oriented one, which is specialized for the specific product. When this specialized application is developed, an interface based on Excel is added to the above basic application. In this section, first, the two types of basic applications with examples are introduced. Next, the specialized applications for specific product is introduced.

BASIC APPLICATION

The two types of Basic applications are developed. One for static and eigen-value analysis is called "Trial_FOA". The other for topology optimization using beam structure is called "TOPODAUKI".

Trial FOA

As shown in Figure 6, an arbitrary model is constructed by inputting the node coordinates and element connectivity as digital data into the Excel sheet. Then the detailed configuration of cross-section is designed like 2-D CAD software, using the special window. It is easy for designers to do it. After setting boundary conditions, the analyses of static and eigen-value are performed. This means simple analysis with respect to arbitrary structures can be performed without using sophisticated commercial software.

The operating procedure of developed FOA application "Trial_FOA" is as follows:

- (1) Input node coordinates and element connectivity into the Excel sheet (Figure 6)
- (2) Create and modify the cross-section of beam element (Figure 7)
- (3) Set boundary conditions (Figure 8)
- (4) Execute static and eigen-value analysis (Figure 9)
- (5) Post-processing results of analysis (Figure 10)

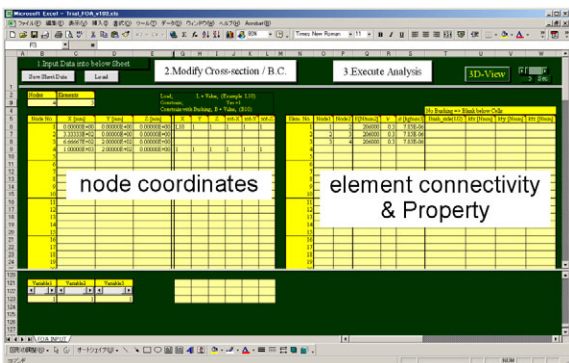


Figure 6. Main sheet of "Trial_FOA"

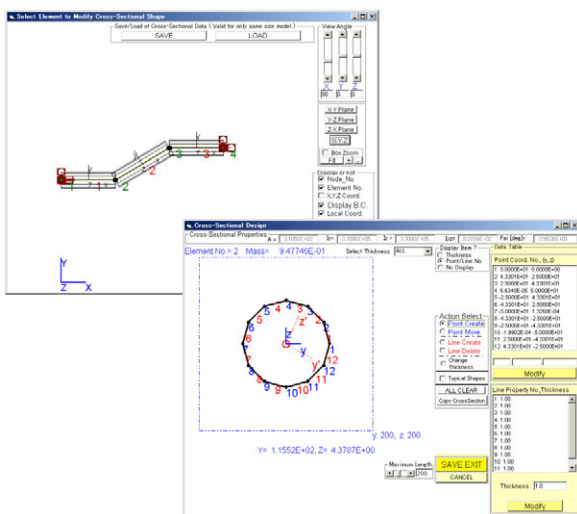


Figure 7. Windows for Create and modify the cross-section

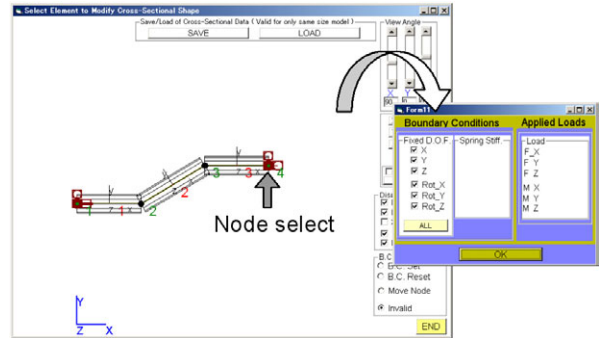


Figure 8. Setting boundary conditions

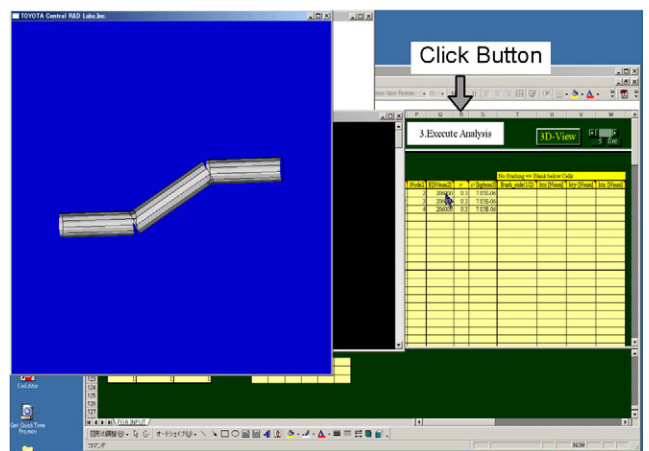


Figure 9. Execute static and eigen-value analysis

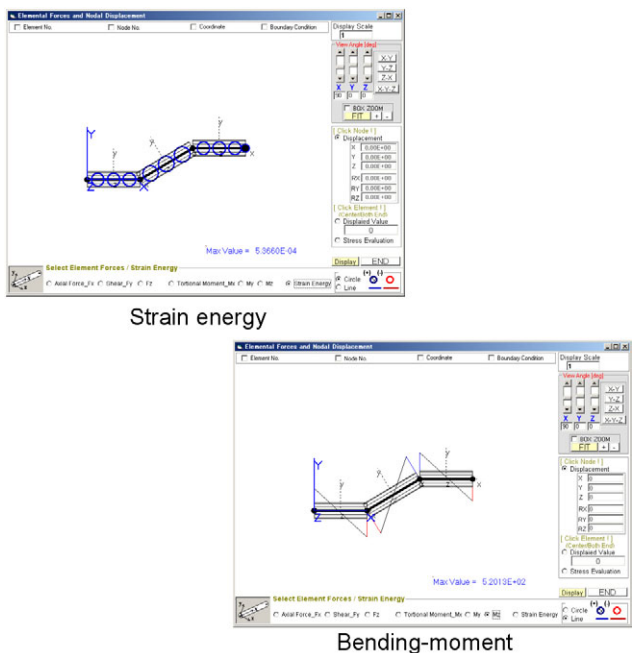


Figure 10. Post-processing Sheets

TOPODAUKI

"TOPODAUKI" is the topology optimization tool, which include pre-post function for easy operation. The purpose of this tool is to easily find out the optimal layout in a conceptual-design stage, using beam components. Then, in order to realize easy operation, the advanced technique for building the grand structure, which is placed in a 3-D design domain, is developed. This technique is to assemble blocks, which are units for creating the grand structure (Figure 11). it has a macro language for performing automation of model creation and analysis from the FOA program included in Excel. Moreover, it can also perform the creation of grand structure and the topology optimization incorporating beam components and panel components, which is not in a design domain but in a non-design domain.

Figure 11-13 shows an example, which has the rectangular domain. In this example, 3-D grand structure can be easily constructed by assembling two blocks like stacking bricks. Figure 12 shows the initial condition. After boundary conditions (Figure 13), the developed topology optimization is performed. As a result, the optimal configuration is obtained as shown in Figure 13. This result indicates that necessary elements, which is linked between the load point and the constrained point, is strengthened and unnecessary elements became much slender. As I mentioned, design engineers can obtain the optimal configuration if only they set a design domain and boundary conditions.

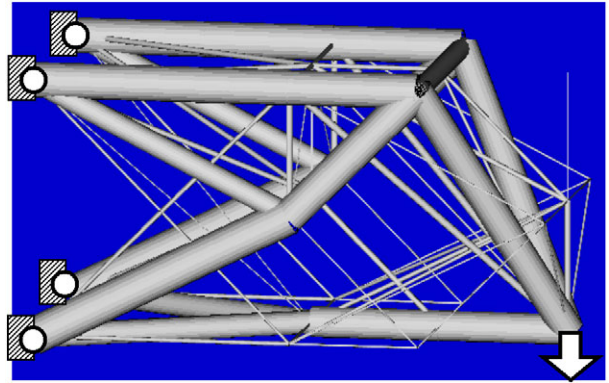


Figure 13. Boundary condition and optimal design

PRODUCT ORIENTED APPLICATION AND EXAMPLES

Stiffness comparison of automotive under body

First, the example with respect to a under body structure, which consists of only frames, is introduced using basic application (Trial_FOA). By the way, most conventional commercial vehicles are divided into three types about under body: (a) Extended Longitudinal, (2) Full Longitudinal, (3) Split Load Path as shown in Figure 14. They are different in the view of load path, which is carried from a front side member to a rear one. Then in this example, the three types of structures are compared.

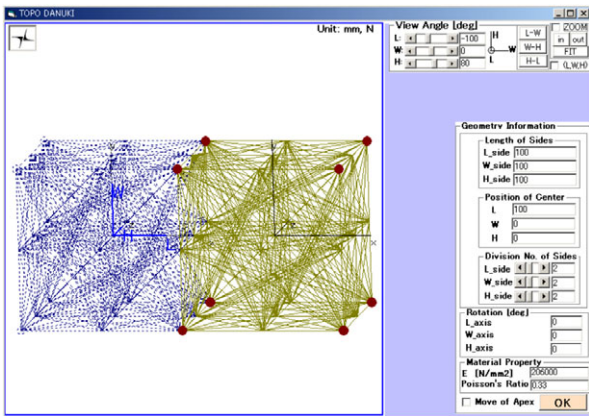


Figure 11. Ground structure production process of "TOPO DANUKI"

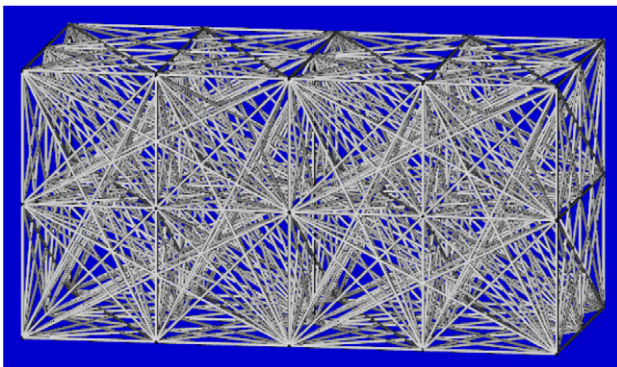


Figure 12. Initial shape of Simple example

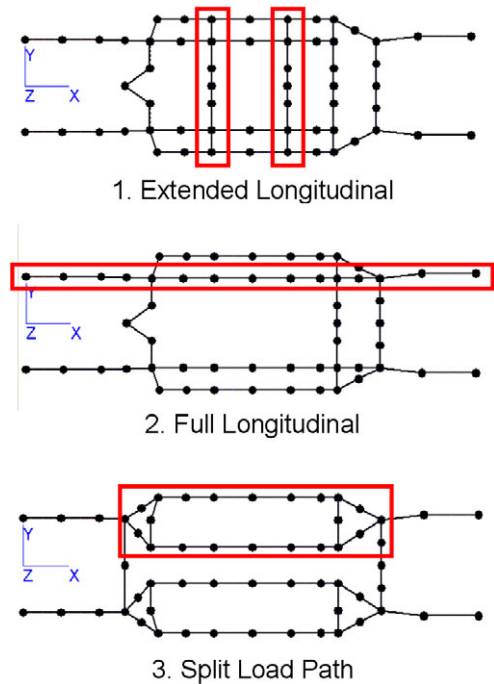


Figure 14. Shape of under body

The model was built on "Trial_FOA". At first, point coordinates and connectivity are written into Excel sheets. In this mode, the beam components, which construct under body frames, have the detailed cross-sectional configuration expressed almost faithfully. These configurations of cross sections are designed using the special window. Then, two points at the end of rear side members are fixed and the axial load is applied at the top point of the front side member on the right side. After that, static analysis is performed (Figure 15).

Comparison of the distribution state of strain energy is shown in Figure 16. Comparison of the displacement at the load point and strain energy is shown in Figure 17. Compared with three types, the type of A distributes strain energy uniformly and the displacement is the smallest. Therefore in this case, it is considered that the type of A is most effective.

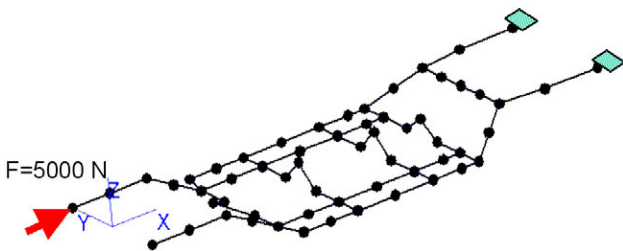


Figure 15. boundary condition by offset load

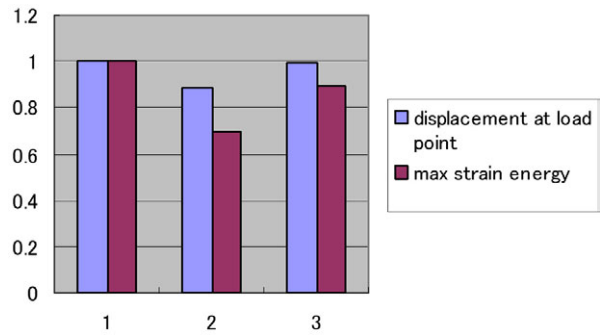


Figure 17. Comparison of displacement and strain-energy

Topology optimization for an under body

Next, the example with respect to an under body structure, which consists of only frames, is introduced using basic application (Topodanuki). This application easily determines an optimal configuration of under body structure by making the interface for constructing a model on Excel.

As shown in Figure 18 and 19, the procedures of this tool are: (1) Select materials, (2) Set parameters, (3) Create and confirm a model, (4) Set max diameter of cross section and max total mass, (5) Set boundary conditions, (6) Select load cases (7) Run analysis, (8) Display results.

This application creates grand structure automatically on the cabin floor of the car which is a design domain. And the boundary condition is also prepared beforehand and analysis is easily performed because a design engineer only chooses the target conditions from the given condition candidates.

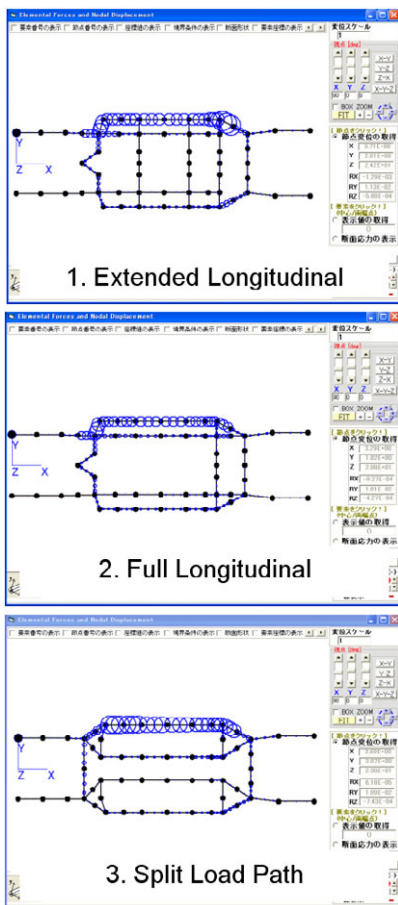


Figure 16. Comparison of strain-energy distribution

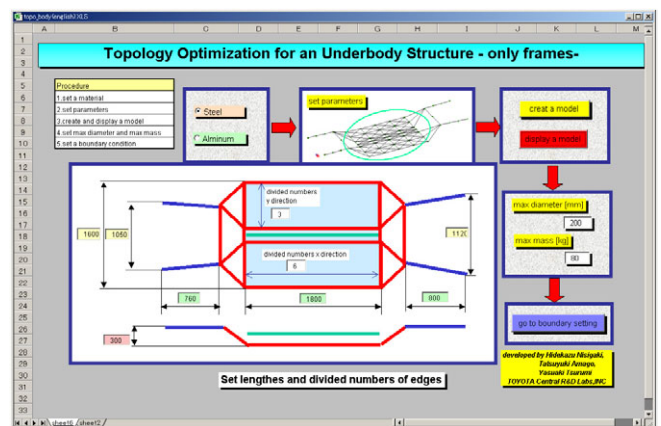


Figure 18. Main sheet by topology optimization for an underbody

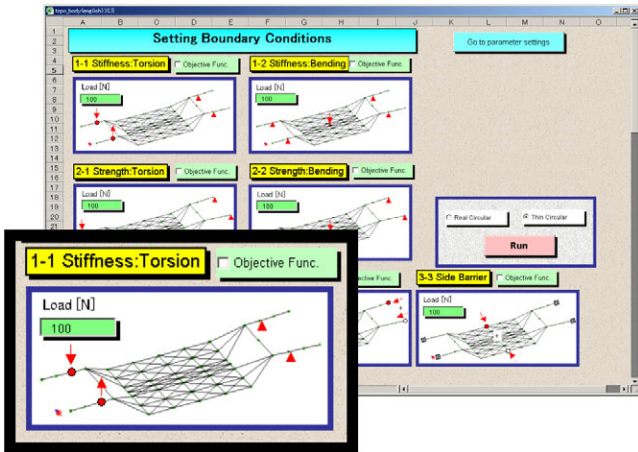


Figure 19. Sheet for boundary condition setting

Figure 20 shows the optimal layout under torsional moment. This result is interpreted as supporting torsional moment by the axial stiffness of remained beams. The axial stiffness is much stronger than the other stiffness in the case of beams. Therefore this result is considered to be optimal under the given constrained condition.

As this example is mentioned, a design engineer can easily obtain an optimal shape in the initial design phase using the developed application.

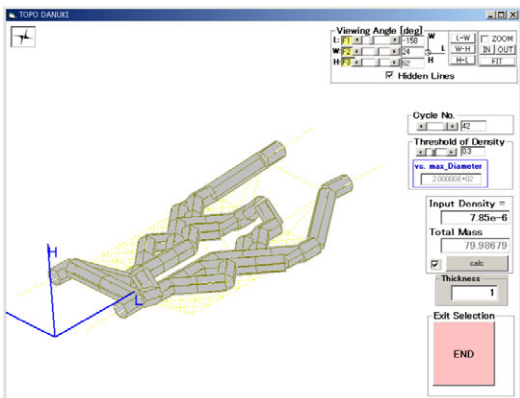


Figure 20. Optimal shape for torsion

AUTOMOTIVE SUSPENSION SYSTEMS

A trailing twist axle rear suspension is widely used in front wheel drive vehicles because of the simple construction and lightweight. It consists of two trailing arms interconnected by a twist beam as shown in Figure 21. They are attached in a rigid manner in order to assure the stability to vertical and lateral forces. The twist beam is the most important component of this suspension. In the case of rolling motion where a relative

displacement between a left wheel and a right one occurs, the twist beam must carry vertical and longitudinal bending moments with minimal deformation, and must simultaneously allow large torsional deformation over its length. In order to satisfy these requirements, a cross-section of the twist beam must be appropriately designed

Here, we show a FOA system for the initial design of the trailing twist axle suspension.

A hierarchal data structure shown in Figure 22 is constructed, and a set of sub-structures are allocated. Figure 23 (a) shows a modeling sheet of the suspension design. By clicking on a beam part in the main sheet, a sub-sheet for the cross sectional analysis appears (Figure 23 (b)). In this sub-sheet, we can graphically draw the cross-sectional shape, and can quickly evaluate its properties. We can see the relation between the shape and its properties by dragging and shortening line segments in this sheet. After setting cross sectional geometries of beam part, design engineers set detailed parameters for each part in a sub-sheet (Figure 23 (c)). Finally, the suspension behaviors such as the alignment behaviors with respect to rolling motion are analyzed in a analysis sheet (Figure 23 (d)).

Thus, suspension design engineers can quickly analyze the suspension behaviors at the initial design phase.

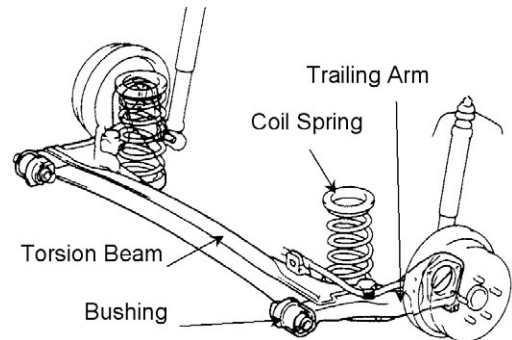


Figure 21. Trailing twist axle suspension.

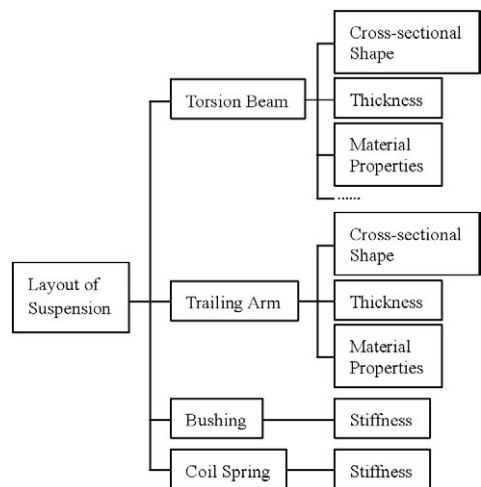
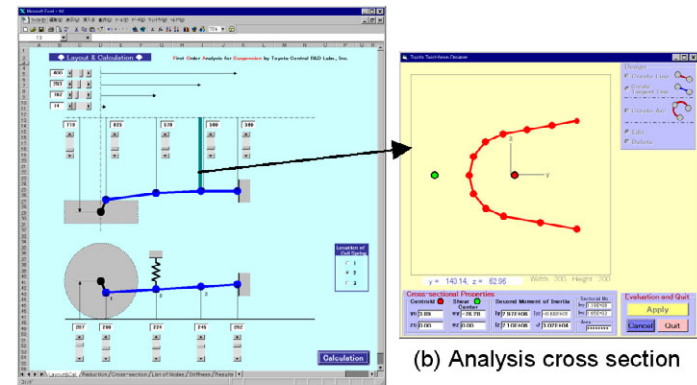
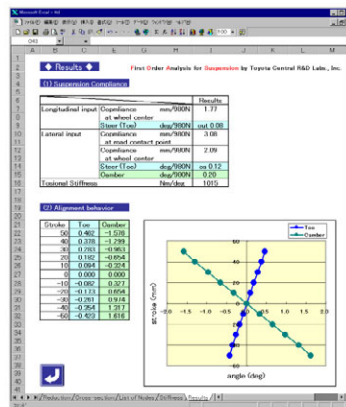


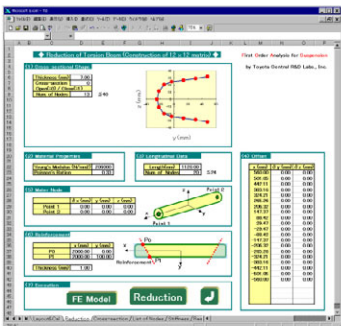
Figure 22. Hierarchal data structure of Automotive suspension.



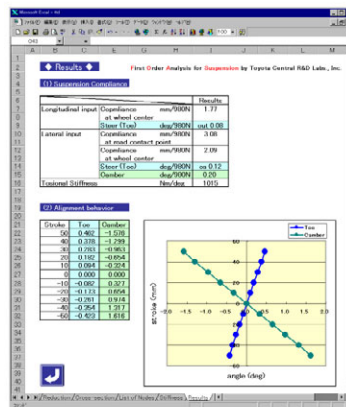
(a) Suspension modeling



(b) Analysis cross section



(c) Detailed parameter setting



(d) Sheet for numerical results

Figure 22. Sheets for suspension design.

FUTURE WORK

We have developed FOA applications under the above concept. Several applications are practically and widely used in each design division. And it comes to be recognized that these are effective and efficient.

However, some requests from users occur, as these applications have been used more widely. Typical requests are that various analysis except static and eigenvalue ones can be treated and more accurate model with satisfying the present ease and speed can be constructed. Of course these requests have to be realized in the conceptual design phase. Then as a first step of the second generation for developing FOA, we have worked on the next topics:

- (1) To construct an advanced joint model
- (2) To treat crashworthiness
- (3) To treat noise & vibration

The detailed contents of the above topics are introduced in Part 2-4 papers.

CONCLUSION

In this paper, we introduce our efforts for developing FOA in the concept design phase.

- (1) Basic concept of FOA is presented. We have developed FOA tools under this concept.
- (2) Two types of basic applications based on the concept of FOA are presented. These tools realize the easy operation and the adequate speed for calculation.
- (3) The specialized applications based on the basic ones are proposed. The availability of its concept is demonstrated by the applications for under body and suspension.

REFERENCES

1. Bendsoe, 1995, "Optimization of Structural Topology, Shape, and Material", Springer-Verlag, Berlin, Heidelberg, pp. 139-180.
2. Bendsoe, M. P. and Kikuchi, N., 1988, "Generating Optimal Topologies in Structural Design Using a Homogenization Method", *Comp. Methods. Appl. Mech. Engrg.*, Vol. 71, pp. 197-224.
3. Dorn, W. S., Felton, L. P. and Greenberg, H. J., 1963, "Automotive Design of Optimal Structures", *J de Mechanique*, Vol.3, pp. 25-52.
4. Howell, L. J. and Chang, D. C., 1981, "Establishing Automobile Structural Design Criteria, Modern Automotive Structural Analysis", Eds. Kamal, M. M. and Wolf, J. A., Van Nostrand Reinhold Co., New York, pp. 35-91.
5. Lemon, J. R., Tolani, S. K. and Klosterman, A. L., 1980, "Integration and Implementation of Computer Aided Engineering and Related Manufacturing Capabilities into Mechanical Product Development Process", *Gi-Jahrestagung*.
6. Nishigaki, H., Nishiwaki, S., Amago, T. and Kikuchi, N., 2000, "First Order Analysis for Automotive Body Structure Design", *Proceedings of DETC'00*
7. Rao, S. S., 1982, "The Finite Element Method in Engineering", Pergamon, pp. 271-294.
8. Sekiguchi, M. and Kikuchi, N., 1999, "Remark on the Mixed Formulation of a Finite Element Stiffness Matrix Based on Clough's Paper in 1960", *Proceedings of the Conference on Computational Engineering and Science, JSCES, Tokyo, Japan, Vol.4, No.1, pp. 131-134.*

CONTACT

The corresponding author of this paper is Tatsuyuki Amago. He is now working at Toyota Central R&D Labs., Inc. His e-mail address is ama@ket.tytlabs.co.jp

First Order Analysis for Automotive Body Structure Design –Part 2 : Joint Analysis Considering Nonlinear Behavior

Yasuaki Tsurumi, Hidekazu Nishigaki, Toshiaki Nakagawa, Tatsuyuki Amago, Katsuya Furuu
Toyota Central R&D Labs.,Inc.

Noboru Kikuchi

The department of Mechanical Engineering at the University of Michigan

Copyright © 2003 SAE International

ABSTRACT

We have developed new CAE tools in the concept design process based on First Order Analysis (FOA). Joints are often modeled by rotational spring elements. However, it is very difficult to obtain good accuracy. We think that one of the reasons is the influence of the nonlinear behavior due to local elastic buckling. Automotive body structures have the possibility of causing local buckling since they are constructed by thin walled cross sections. In this paper we focus on this behavior. First of all, we present the concept of joint analysis in FOA, using global-local analysis. After that, we research nonlinear behavior in order to construct an accurate joint reduced model. (1) The influence of local buckling is shown using uniform beams. (2) Stiffness decrease of joints due to a local buckling is shown. (3) The way of treating joint modeling considering nonlinear behavior is proposed.

INTRODUCTION

We have developed new CAE tools based on First Order Analysis (FOA) since 1999(Nishiwaki[1]). FOA tools are used on the concept design development process. The basic ideas of FOA are:

- 1) Graphic user interface for automotive design engineers using Microsoft Excel.
- 2) Use of sophisticated formulation based on the theory of mechanics of materials.
- 3) A topology optimization method using functions oriented elements such as beam elements.

Using the above ideas, design engineers can easily utilize FOA tools and determine basic layouts based on structural mechanics without spending much time. Therefore FOA tools have come to be very significant in the concept design process.

On the other hand, as FOA has used more widely and deeply, advanced functions to solve various problems are required. Especially a problem with respect to joints is one of the most significant one for automotive body structures. For example a global torsion stiffness of a body-in-white greatly depend on joint flexibilities. Therefore their behavior about joints must be accurately estimated in the analysis. Generally shell elements are used in order to construct finite element models. In the concept design phase, where FOA tools are used, these shell element models of joints are replaced with rotational spring element models (EI-sayed,M.E.M[2]) whereas rails, pillars and frames are modeled with beam elements to simplify the analysis. However, it is very difficult to obtain the good accuracy using these spring elements. It is considered that there are two reasons. One is the transformation error from shell element models to spring element models (Kim[3]). The other is a bad effect of nonlinear behavior due to local elastic buckling. Various studies about the former one are addressed and a few different models are used (Kim[4],Lee[5]). However no studies about the latter one have ever been heard, as far as I know. Automotive body structures have the possibility of casing local elastic buckling since they are constructed by thin walled cross sections. Once local elastic buckling occurs, stiffness decreases and the yield point becomes lower. Therefore it is very important to consider this buckling. This behavior cannot also be evaluated even if joint models are constructed using detailed linear shell elements.

First of all, in this work we present the concept of joint analysis in FOA. We propose to use Global-Local Analysis to obtain both a good accuracy and an adequate speed for analyzing. For realizing this concept, several unknown problems must be resolved such as how to construct a good reduction model for static and dynamic behavior, etc.

As a first step to resolve some unknown problems, we focus on the nonlinear behavior due to local elastic buckling in order to see if we should use a nonlinear model. Our approach is:

- (1) The influence of local buckling is shown using uniform beams. Nonlinear behavior is predicted using a beam elements, whose cross section properties are calculated based on the theory of effective width (Marin and Diewald[6]).
- (2) Stiffness decrease of joints due to local elastic buckling are shown with respect to in-plane and out-plane bending. It is hard to predict nonlinear behavior without using nonlinear analysis.
- (3) The two ways of treating how to construct a joint model considering nonlinear behavior is proposed. One is to move a buckling frequency from the present point to the upper point, as much as possible. The other is to use the nonlinear spring constant in the global analysis.

THE CONCEPT OF JOINT ANALYSIS IN FOA

We use Global- Local analysis in order to obtain both a good accuracy and an adequate speed for analyzing in FOA. This way is shown as followings:

- (1) Joint configurations are exactly modeled using shell elements for local analysis. Using this model, necessary performance such as stiffness, vibration and strength is estimated. Nonlinear analysis in addition to linear one is performed (Figure 1(b)).
- (2) A reduced model based on the above results is constructed for global analysis (Figure 1(b)).
- (3) Databases about typical joint configurations are constructed repeating these procedures from (1) through (2) (Figure 1(c)).
- (4) The reduced models of the joints are inserted in a global model and global performance is estimated. This analysis is simple and fast. The joint flexibility of the reduced model is optimized for satisfying a target performance (Figure 1(d),(e)).
- (5) In the local analysis, the joint configuration (layout) is optimized based on the optimized reduced joint flexibility. In this optimization process, the database is referred and the optimal layout will be found out (Figure 1(f)).

This way is very significant in FOA. But we have to recognize right behavior of joints in order to construct a good reduced model. As a first step we focus on the nonlinear behavior due to local elastic buckling.

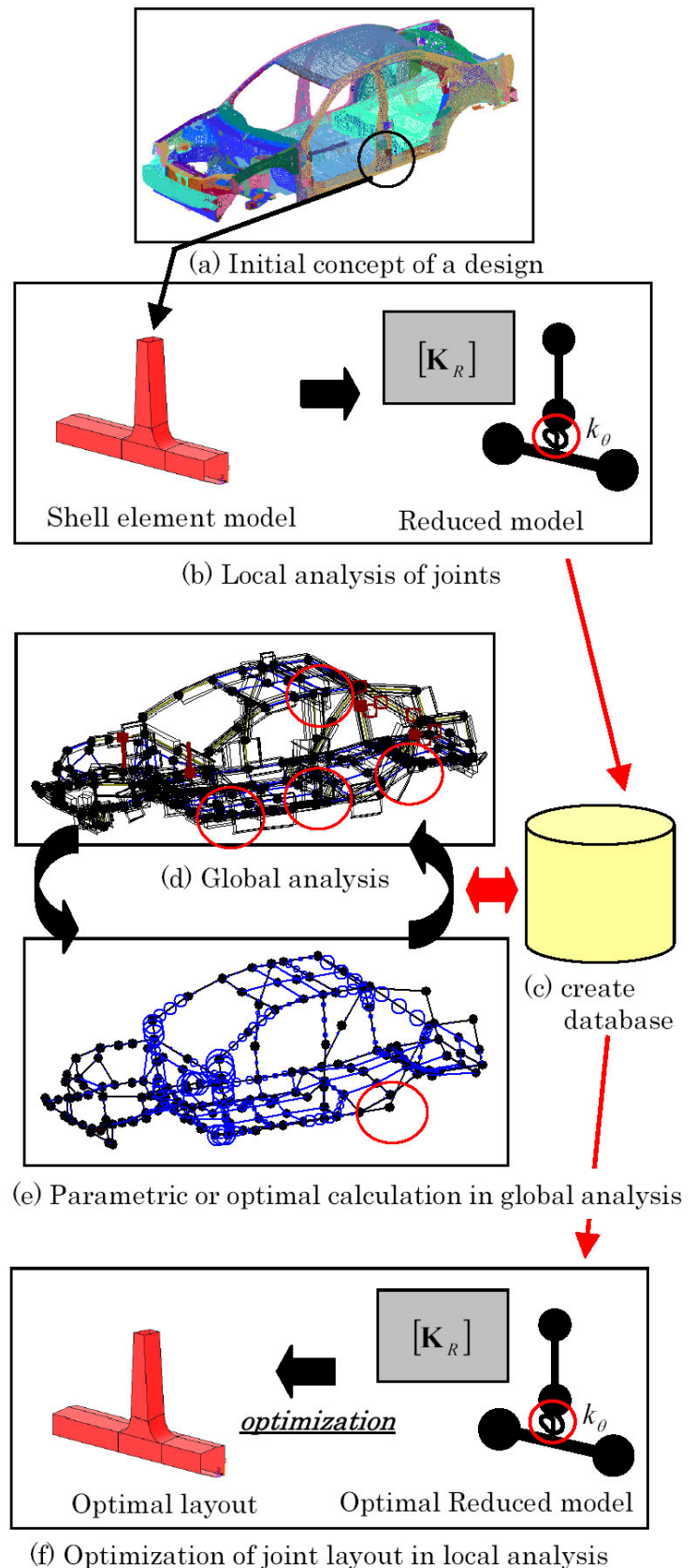


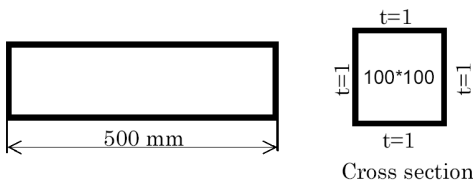
Figure.1 The concept of global-local analysis

INFLUENCE OF LOCAL ELASTIC BUCKLING IN THE CASE OF UNIFORM BEAMS

Before analyzing joints, basic research of local elastic buckling is performed using uniform beam structures. In automotive body structures, individual elements of frame structural members are usually thin and the width-to-thickness ratios are usually large. Then thin elements may buckle locally at a stress level lower than the yield point of steel when they are subjected to compression in flexural bending, axial compression, shear, or bearing (Yu[7]). Stiffness decrease is verified using nonlinear simulation. Moreover this behavior is predicted based on the theory of effective width.

ESTIMATION USING SHELL ELEMENT MODELS

In this section, buckling behavior is calculated using shell element models. We use ANSYS ([8]) for this analysis. Nonlinear analysis is performed including initial deflection that is obtained by 1-th buckling eigenvalue analysis. As shown Figure 2, the uniform box beam element is used with respect to two types of boundary condition, (1) axial compression condition, (2) vertical force condition.



$$E(\text{young modulus}) = 203000 \left(N/mm^2 \right)$$

$$\nu(\text{poisson ratio}) = 0.3$$

$$\sigma_y(\text{yield stress}) = 269 \left(Mpa \right)$$

Figure.2 Test model of the uniform box beam

Axial compression condition

Fig.3 shows the deformation at the local elastic buckling load. As shown Fig.4, the local elastic buckling occurred at the lower point ($F=3.16e4[N]$) than the yield point ($F=4.52e4[N]$). Stiffness decrease in the elastic domain is confirmed after causing the local elastic buckling. In this case, the axial stiffness became about half of the initial one. This is the significant problem. If this axial stiffness is estimated without considering the influence of the local buckling, the weaker structure than you thought is designed.

Vertical force condition

Figure 5 shows deformation at the local elastic buckling load. As shown Fig.6, the local elastic buckling occurred at the lower point ($F=3.82e3[N]$) than the yield point ($F=4.49e3[N]$). Stiffness decrease in the elastic domain is confirmed after causing the local elastic

buckling. The bending stiffness did not change so much. In this case the influence of buckling is small.

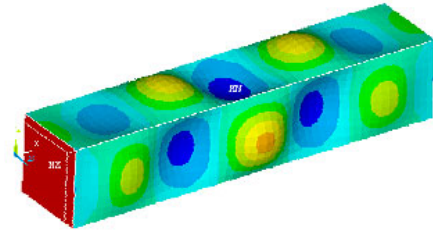


Figure.3 Deformation at the axial load ($F=3.16e4[N]$)

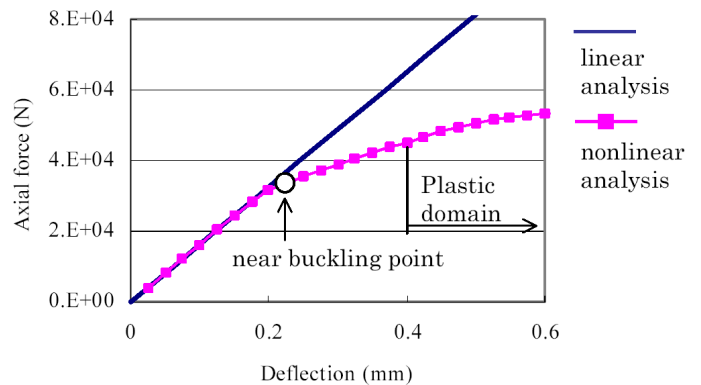


Figure.4 Influence of local elastic buckling under the axial compression condition

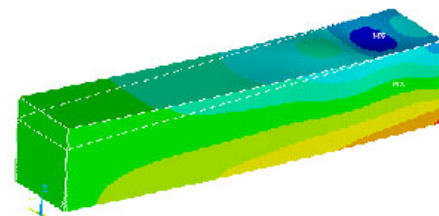


Figure.5 Deformation at the vertical force ($F=3.82e3[N]$)

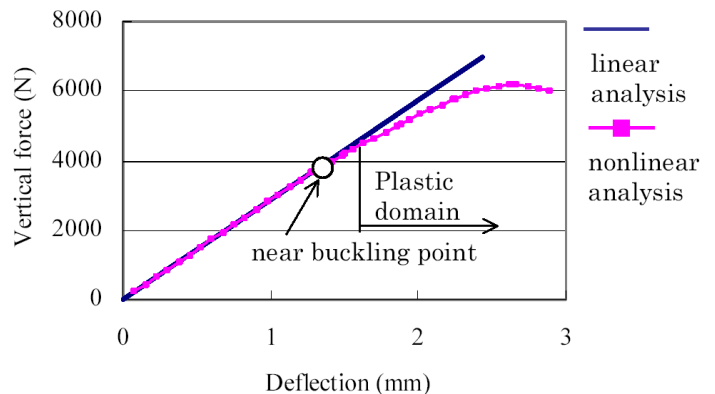


Figure.6 Influence of local elastic buckling under the vertical force condition

This is because only one surface near the rigid point is buckled. However this uniform beam with the buckling trends to reduce the strength compared with the structure, whose local elastic buckling eigenvalue is bigger than the yield point. Therefore this behavior is also the significant problem.

HOW TO TREAT LOCAL BUCKLING IN FOA

In beam structures, the influence of local elastic buckling can be estimated based on the theory of effective width. In this section, effective width under the axial compression condition is calculated and the reduction in stiffness is predicted.

The theory of effective width

The above beam model has uniformly compressed stiffened elements. The effective width (=b) of these elements is determined (Marin and Diewald[6]) as followings:

$$\begin{aligned}
 b &= w & \text{when } \lambda \leq 0.673 \\
 b &= \rho w & \text{when } \lambda > 0.673
 \end{aligned}
 \tag{1}$$

where w = width of the element

$$\rho = \frac{1 - 0.22}{\lambda}
 \tag{2}$$

where λ is a slender factor determined by

$$\lambda = 1.052 \left(\frac{w}{t} \right) \sqrt{\frac{f}{E}}
 \tag{3}$$

where f = stress in the element
 E = Young's modulus of the element
 k = plate buckling coefficient
 t = thickness of the element

- (1) Compute the normal stress distribution based on a given stress level assuming all the segments are fully effective.
- (2) Based on the computed stress distribution and the segment type, calculate effective widths of each segment (referred to Eqn (1)-(3)).
- (3) Calculate the cross section properties of the section based on the effective portion of each segment.
- (4) The above procedures are repeated until the cross section properties converge.

Then if the next convergence condition is assumed,

$$b_n \rightarrow b \quad \text{if } n \rightarrow \infty$$

where b_n = effective width at n -th cycle

we can obtain the effective width using Eqn (5) without repeating (1)-(4).

$$\begin{aligned}
 b &= \left(\frac{1}{\frac{B}{w} + \frac{0.22}{B}} \right) \\
 B &= 1.052 \left(\frac{w}{t} \right) \sqrt{\frac{F}{4Ekt}}
 \end{aligned}
 \tag{5}$$

In the case of the axial compression condition, the total effective width is calculated as shown Figure 7. The influence of local elastic buckling is seen from the point, which doesn't reach the local buckling force.

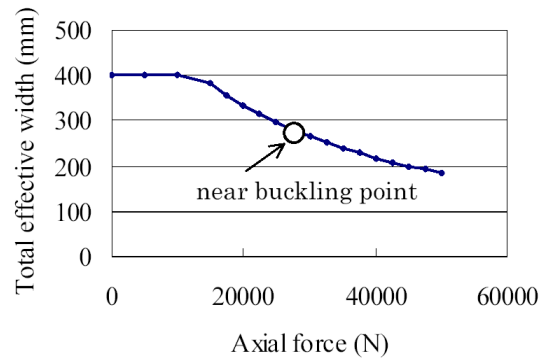


Figure.7 Effective width under the axial compression

The prediction of the influence to stiffness

The axial stiffness is calculated using the cross section properties of the section based on the effective portion. However not all sections have the effective width. As Figure 8 is shown, the portion with the effective width and the rest with the fully effective width exist. Then we use Eqn (6) in order to calculate the axial stiffness. Figure 9 shows the results of three different methods. As a result, the result based on the theory of effective width is well consistent with the result of nonlinear analysis by ANSYS. That is to say, we can predict the influence of local elastic buckling without complicated nonlinear analysis. In the case of the vertical force condition, we can also predict using the same method.

The behavior of local elastic buckling has the possibility of giving thin walled beam structures a big damage with respect to stiffness and strength. Design engineers have to consider these problems in the concept design process. However they don't perform complicated simulation using Finite Element (FE) commercial software. Therefore the above method is greatly effective. It enables the estimation of nonlinear behavior without complicated analysis. Moreover this nonlinear behavior cannot be obtained by linear analysis even if detailed shell element models are used.

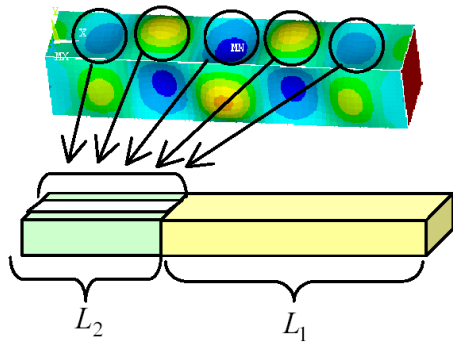


Figure.8 The estimation of stiffness by buckling

$$K = \frac{F}{u} = \frac{EA_1A_2}{L_1A_2 + L_2A_1}$$

$$L_2 = nb$$

where

K = axial stiffness

F = axial compression force

u = axial deflection

A_1 = cross section area at the fully effective width

A_2 = cross section area at the effective width

L_1 = length at the fully effective width

L_2 = length at the effective width

b = effective width

n = number of mode

(6)

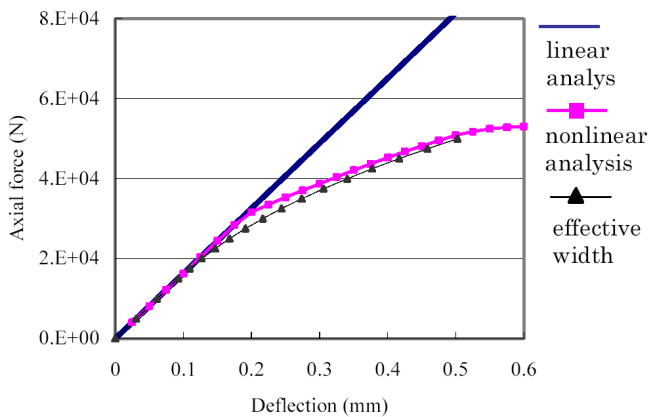
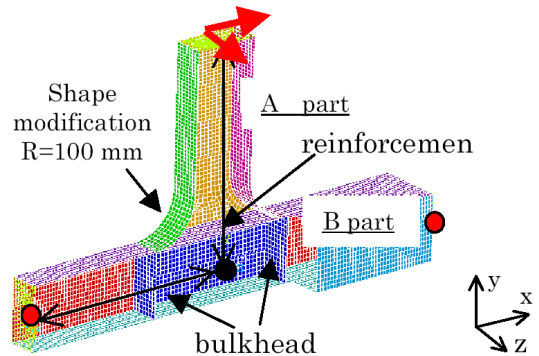
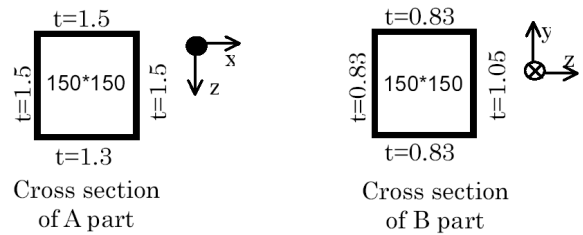


Figure 9 the comparison among three methods

INFLUENCE OF LOCAL ELASTIC BUCKLING IN THE CASE OF JOINT STRUCTURES

In this section, the influence of local elastic buckling with respect to joint structures is studied. The influence with respect to uniform beams is estimated by the method based on the theory of effective width. However, it is unknown if this method can be applied to joint structures. Then we work on the analysis of basic joint structures (Figure 10). The two type of conditions, (1) in-plane bending (2) out of plane bending, and three typical modifications for increasing stiffness, (a) bulkhead

(b) reinforcement (c) shape modification in addition to an initial shape are considered. Nonlinear analysis is performed including initial deflection that is obtained by buckling eigenvalue analysis.



500 mm Rigid point

$$E(\text{young modulus}) = 203000 \left(N/mm^2 \right)$$

$$\nu(\text{poisson ratio}) = 0.3$$

$$\sigma_y(\text{yield stress}) = 400 \text{ (Mpa)}$$

Figure 10 Test model

IN-PLANE BENDING

Figure 11 shows the deformation of the initial shape at the local elastic buckling load. As shown Figure 12, this deformation by the local elastic buckling occurred at the lower point ($F=4.55e3[N]$) than the yield point ($F=6.07e3[N]$) mainly in the joint. Stiffness decrease in the elastic domain is confirmed after causing the local elastic buckling. In this case, the bending stiffness became about half of the initial one. This behavior cannot be predicted using the theory of effective width because this buckling is not a general plate one.

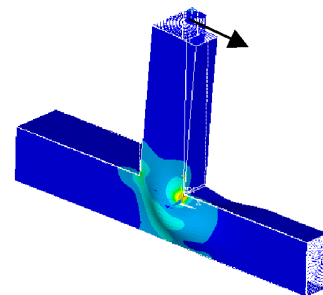


Figure.11 Deformation at the vertical force ($F=4.55e3[N]$)

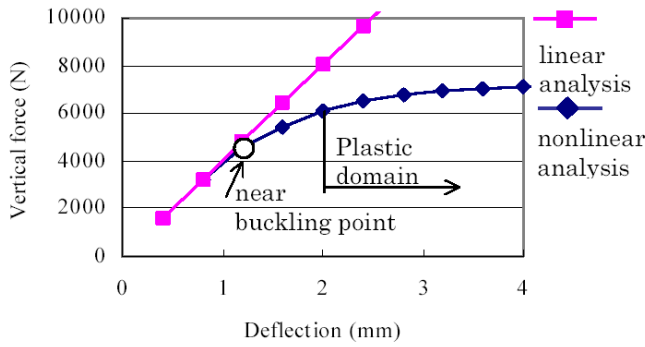


Figure.12 the Influence of the local elastic buckling under the initial condition

Table 1 shows the rate of stiffness decrease. In all of cases, the deformations by the local elastic buckling occur at the lower point than the yield point (Figure 13) and stiffness decrease in the elastic domain is confirmed after causing the local elastic buckling. The reduction rate in the case (a) is the smallest. This means the influence of this buckling is very small. The reason is that in the case (a), the buckling mode is different from the others. The buckling mode, which occurs not in the joint, is the plate buckling one on the surface of B part (Figure 14). The other modes such as figure 11 are the shear buckling modes in the joint. It is considered the shear one badly affects decrease of bending stiffness.

Table 1. Comparison stiffness in the case of in-plane bending

	Initial (N/mm)	Reduced (N/mm)	Reduction rate %
initial	4021	1909	53%
(a) bulkhead	5160	4490	13%
(b) reinforcement	4456	2525	43%
(c) shape modified	5670	3760	34%

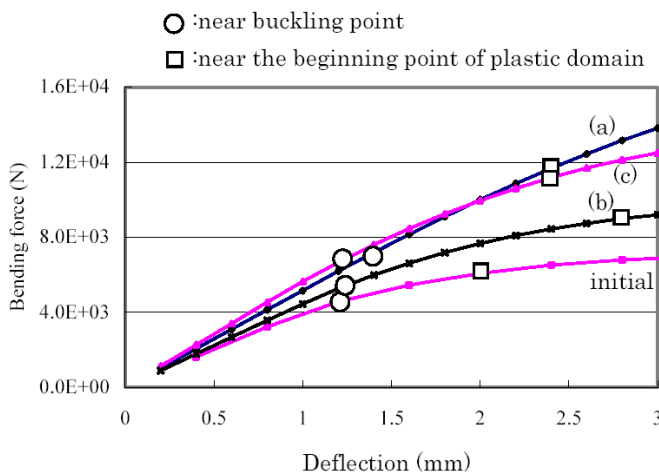


Figure.13 Comparison among different cases

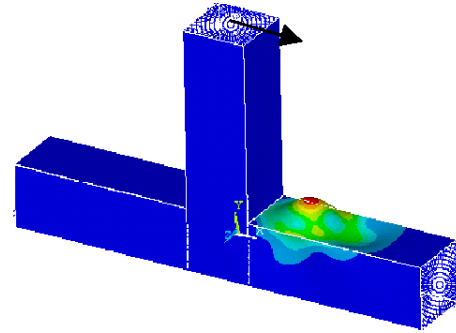


Figure.14 Buckling mode (1)-(a) ($F=6.285e3[N]$)

OUT OF PLANE BENDING

Figure 15 shows deformation of the initial shape at the local elastic buckling load. As shown Figure 16, this deformation by the local elastic buckling occurred at the lower point ($F=2.154e3[N]$) than the yield point ($F=4.14e3[N]$). Stiffness decrease in the elastic domain is confirmed after causing the local elastic buckling. In this case, the bending stiffness became about 60 % of the initial one. This decrease is affected by two different type of buckling modes (as shown Figure 17). These are like the plate buckling mode and the share one. However it is difficult to predict this behavior using the theory of effective width since they are not simple ones.

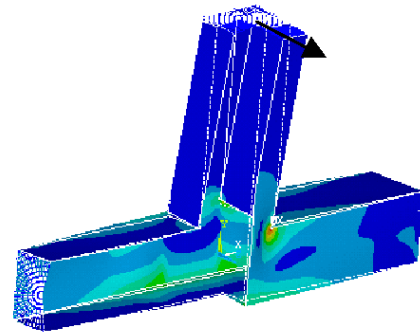


Figure.15 Deformation at the vertical force ($F=2.54e3[N]$)

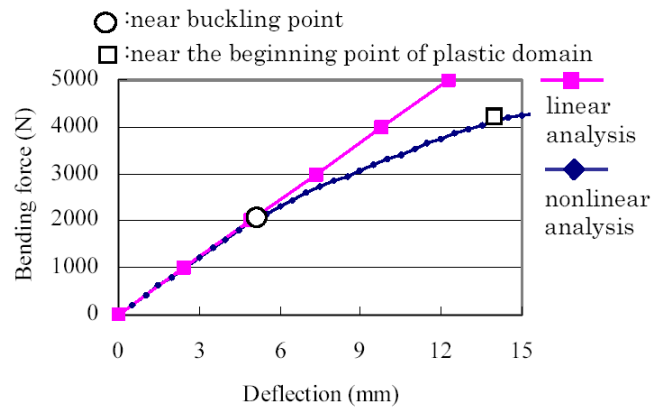


Figure.16 Influence of local elastic buckling under the initial condition

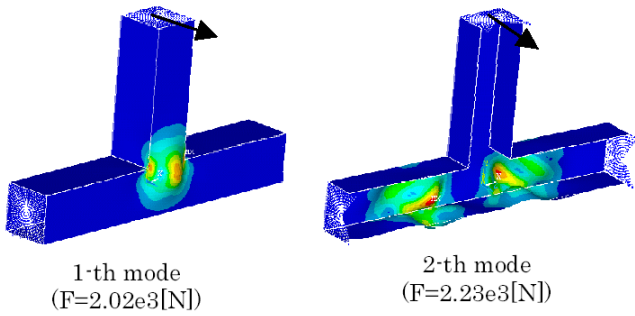


Figure.17 Buckling mode

Table 2 shows the rate of stiffness decrease. In all of cases, the deformation by the local elastic buckling occurs at the lower point than the yield point (Figure 18) and stiffness decrease in the elastic domain is confirmed after causing the local elastic buckling. Each of the reduction rates is the larger than 25 %. The first modes of (a), (b), (c) are similar to the second mode of the initial shape (Figure 17). They belong to torsional buckling modes by a torsional action. It is considered the torsional buckling mode on the surface of B part badly affects decrease of bending stiffness.

Table 2. Comparison stiffness in the case of in-plane bending

	Initial (N/mm)	Reduced (N/mm)	Reduction rate %
initial	407	232	43%
(a) bulkhead	1560	1080	31%
(b) reinforcement	427	317	26%
(c) shape modified	500	367	27%

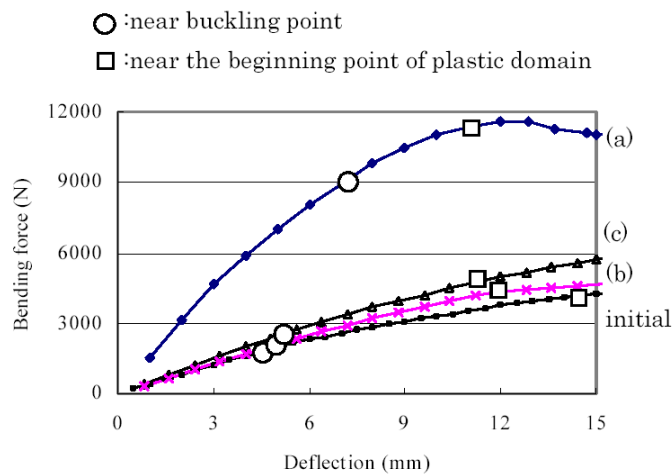


Figure.18 Comparison among different cases

THE WAY OF CONSTRUCTING JOINT MODELS

As I mentioned in the previous section, the buckling behavior of joint structures cannot be easily

estimated using the theory of effective width. Because this buckling mode is a shear buckling and a torsional buckling, not a general plate buckling. However this behavior have to be predicted in the concept design process, in order to restrict the stiffness decrease.

On the other hand, we present global-local analysis. At first, we construct joint detailed shell element models about typical joint structures of automotive body and perform various analyses moving design parameters, such as static, dynamics, nonlinear etc. After that, joint models are reduced considering various characteristics obtained by the above analyses.

In this section, after presenting how to construct the liner reduced model using a scalar spring element, we present two type of ways of treating the nonlinear behavior based on local elastic buckling, (1) to find out a joint structure, which does not cause the elastic buckling before the yield point in the local analysis as much as possible and (2) to construct a reduced model including the influence of the local elastic buckling such as a nonlinear spring element.

THE LINEAR REDUCED MODEL

As shown Figure 19, T joint model based on shell elements is constructed. In addition to it, T joint model based on beam elements with rotational spring elements is constructed (Figure 20). The translation connection between two beams is rigid. The latter model is the reduced model of the previous one.

It is assumed that the both edge points of B part are fixed and each of in-plane and out of plane bending load is applied at the edge point of A part. These are unit loads. The rotational spring constant k is calculated so that the displacement of point 3 in the beam model is equal to the one in the shell model.

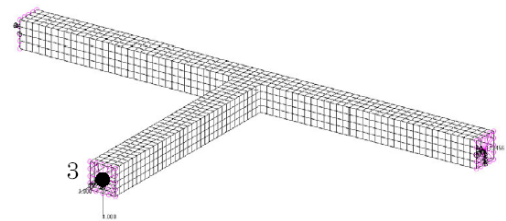


Figure 19 Joint model based on shell elements

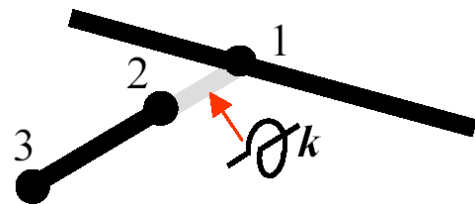


Figure 20 Joint model based on beam elements

The relation among three points (1,2,3) in the beam model with a rotational spring is written as

$$\begin{bmatrix} k'_{11} & k'_{12} & k'_{13} \\ k'_{21} & k'_{22} & k'_{23} \\ k'_{31} & k'_{32} & k'_{33} \end{bmatrix} \begin{Bmatrix} u_1 \\ u_2 \\ u_3 \end{Bmatrix} = \begin{Bmatrix} 0 \\ 0 \\ 1 \end{Bmatrix}$$

$$(k'_{11} = k_{11} + k, k'_{22} = k_{22} + k, k'_{12} = k'_{21} = k_{12} - k)$$

where k_{ij} is a component of the reduced stiffness matrix
 k is a rotational spring constant
 u_1, u_2 is rotational displacements
 u_3 is a displacement

----- (7)

If the displacement at point 3 in the shell model is u^* , k is given as

$$k = \frac{\begin{pmatrix} -k_{12}^2 + k_{11}k_{22} + k_{11}k_{23}^2u^* + k_{12}^2k_{33}u^* \\ -k_{11}k_{22}k_{33}u^* + k_{13}^2k_{22}u^* - 2k_{12}k_{13}k_{23}u^* \end{pmatrix}}{\begin{pmatrix} -k_{11} - 2k_{12} - k_{22} - k_{23}^2u^* + k_{11}k_{33}u^* \\ +2k_{12}k_{33}u^* + k_{22}k_{33}u^* - k_{13}^2u^* - 2k_{13}k_{23}u^* \end{pmatrix}}$$

----- (8)

if $u_3 = u^*$

The linear reduced model of joint modulus in global analysis is obtained as the rotational spring constant. This reduced data is saved in database.

THE WAYS OF TREATING NONLINEAR BEHAVIOR BY LOCAL ELASTIC BUCKLING

In the case of local analysis

The influence of local elastic buckling is studied using the shell model (Figure 19) in the local analysis. If the stiffness decrease is confirmed, we try to find out a joint structure, which does not cause the elastic buckling before the yield point as much as possible. Then as one of results in database, both initial stiffness and modified one by elastic local buckling like Table 1 and 2 are saved.

When a design engineer determines a joint layout, he can obtain a better structure, which isn't badly affected by a local elastic buckling, if he uses this database. He can also calculate another better one from interpolation data, which will be obtained using response surface method.

I would like to show our idea of joint structures that are not badly affected by local elastic buckling.

Shear load is applied on the side surfaces of joints under an in-plane bending force condition. This load causes a shear buckling. In order to restrict it, supporting shear load is important. Inserting bulkhead is good as shown Table 1 (a).

Torsional moment is applied on the surfaces of joints under an out of plane bending force condition. This moment causes a torsional buckling. In order to restrict it, increasing rotational stiffness is important. Figure 21 shows an additional example. In this model, the linear stiffness is made increase by bulkhead. Next, two types of means for local elastic buckling are performed; shape modified and thickness increase. As a result, the initial stiffness is 1600 [N/mm] and the modified stiffness after buckling is 1300 [N/mm]. The reduction rate becomes much smaller (19 %).

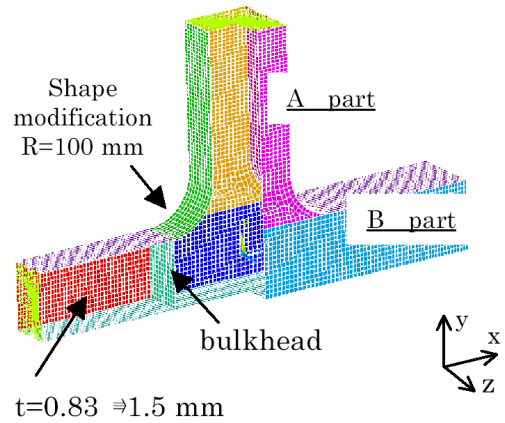


Figure.21 The modified structure

In the case of global analysis

A simple model, which mainly consists of beam elements, is utilized in global analysis. It is so fast and easy to calculate. In this model, joint models are reduced. Then we propose to construct a reduced nonlinear model and perform nonlinear analysis including the influence of the local elastic buckling in joint structures. We think this calculation is not so time-consuming.

As shown Figure 22, we present to approximate the nonlinear stiffness using a bilinear line (K_1, K_2). After that, spring constants (k_1, k_2) is calculated using Eqn (8). We think the nonlinear behavior like Figure 22 can be simulated using the reduced model with a nonlinear spring constant.

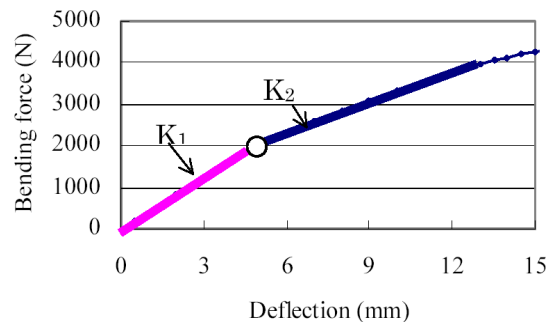


Figure.22 Approximation of the stiffness (the initial model under out of plane load)

FUTURE WORK

In this section, we show only the concept of treating the nonlinear behavior. As a next step, we would like to create practical database including the influence of the nonlinear behavior after verifying the above concept.

CONCLUSION

We have researched how to design joint structures in the concept design phase using simulation. As a first step, we mainly studied the nonlinear behavior of joints using simple basic structures.

- (1) We propose to use the concept of global-local analysis for obtaining a good accuracy and an adequate speed.
- (2) The stiffness decrease by local elastic buckling is confirmed using uniform beams. Moreover we simulate the behavior using the theory of effective width.
- (3) The stiffness decrease by local elastic buckling is also confirmed in joint structures. Shear buckling and torsional buckling causes this behavior.
- (4) We propose the way of constructing joint models. We present two type of ways of treating the nonlinear behavior based on local elastic buckling:

to find out a joint structure, which does not cause the elastic buckling before the yield point in the local analysis

to construct a reduced model including the influence of the local elastic buckling such as a nonlinear spring element.

REFERENCES

1. Nishigaki, H., Nishiwaki, S., and Kikuchi, N., 2001, "First Order Analysis – New CAE Tools for Automotive Body Designers", Proceedings of SAE 2001 World Congress, Detroit, USA, 2001-01-0768
2. El-sayed, M. E. M., 1989, "Calculation of joint spring rates using finite element formulation", Computers and Structures 33(4), 977-981
3. Kim, Y. Y., Yim, H. J., and Kang, J.H., 1995, "Reconsideration of the joint modeling technique: in a box-beam T-joint", SAE, 951108, pp.275-279
4. Kim, Y. Y., and Kim, H. J., 2002, "New accurate efficient modeling techniques for the vibration analysis of T-joint thin-walled box structures", Solid and Structures, Elsevier Science Ltd., 39(2002), 2893-2909
5. Lee, K., and Nikolaidis, E., 1992, "A two-dimensional model for joints in vehicle structures", Computers and Structures, 45(4), 775-784
6. Marin, D. C. and Diewald, T. E., 1998, "Automotive Steel Design Manual", American Iron and Steel Insutitute and Auto/Steel Partnership, pp.3.1.1-3.1.52.
7. Wei-Wen Yu., 1972, "Cold-formed Steel Structures", Mcgraw-hill book company
8. 2003, "Seminar note of ANSYS structural nonlinear analysis", cybernet system

CONTACT

The corresponding author of this paper is Yasuaki Tsurumi. He is now working at Toyota Central R&D Labs., Inc. His e-mail address is e0927@mosk.tytlabs.co.jp.

First Order Analysis for Automotive Body Structure Design - Part 3: Crashworthiness Analysis Using Beam Elements

Hidekazu Nishigaki

Toyota Central R&D Labs., Inc.

Noboru Kikuchi

The University of Michigan

Copyright © 2003 SAE International

ABSTRACT

We have proposed *First Order Analysis* (FOA) as a method, which the engineering designers themselves can use easily in an initial design stage. In this paper, we focus on the crashworthiness, and present the method to predict the collapse behavior of the frame member. This method is divided into two parts. Those are (1) collapse analysis under loading conditions of combined axial force and bending moment to the cantilever, and (2) collapse analysis of structural member considering the previously obtained moment – rotation angle relationship using the beam element. In comparison with the results according to the detailed Finite Element Analysis (FEA) model, effectiveness and validity of this method are presented.

INTRODUCTION

In recent years, Computer Aided Engineering (CAE) has been remarkably developed, and has spread widely. Consequently, before making prototypes, quantitative prediction of performance of automobiles is becoming to some extent possible. Structure with more sufficient performance can be proposed based on the results of CAE. Since the importance of CAE has been increasing, the CAE specialist has shifted to more advanced analysis – material and geometrical nonlinear problems, multi-field problems, for example. As CAE tool for the engineering designers which can directly use a CAD model has been put in practical use, in many linear problem cases, engineering designers have come to perform structure examination using CAE in the drawing stage. By the way, in the initial design stage, a novel proposal and substantial change for layout of the automobile body structure are comparatively easy. Generally, in this initial design stage, CAE analysis using a rough model or the modified model of a vehicle of an old type has been performed easily, and recognized as an effective method.

On the other hand, although the calculation using theory of mechanics of materials and the simple analysis using beam element are unsuitable for quantitative examination, they are effective in an understanding of a phenomenon by the reason for simplifying an object based on designer's know-how. Moreover, change for layout of the automobile body structure is very easy. Therefore, in the examination stage before creating a CAD drawing, it is considered effective methods. And also when evaluating and considering the result of CAE, it helps to acquire more knowledge.

We have proposed *First Order Analysis* (FOA) as a method, which the engineering designers themselves can use easily in an initial design stage (Nishigaki [1]). This method makes it the main purpose to understand the characteristic of a subject and to assist thinking and consideration of an engineering designer in the conceptual design stage before carrying out CAE. The basic concepts of FOA include (1) graphical user interfaces for the engineering designers using Microsoft/Excel (2) use of well understandable formulations based on the theory of mechanics of materials.

By the way, responding to high demand for weight efficient and crashworthy design of automobile bodies, many studies on thin-walled members subject to large deformation have been carried out. Abramowicz [2] and Kecman [3] studied the problem of a deep bending collapse of open and closed section, respectively. Both authors followed the so-called kinematic method of plasticity, which involved determination of a suitable folding mechanism with stationary and/or moving plastic hinges. Kecman, Sadeghi and Vignjevic [4] had developed a compound beam element with varying joint and hinge moment-rotation curves and implemented into the public version of program DYNA-3D for the purpose of responding to a demand in the early design stages. This beam combines the existing Belytschko-Schwer beam element with rotary springs having very nonlinear moment-rotation curves in the elastic-plastic and deep

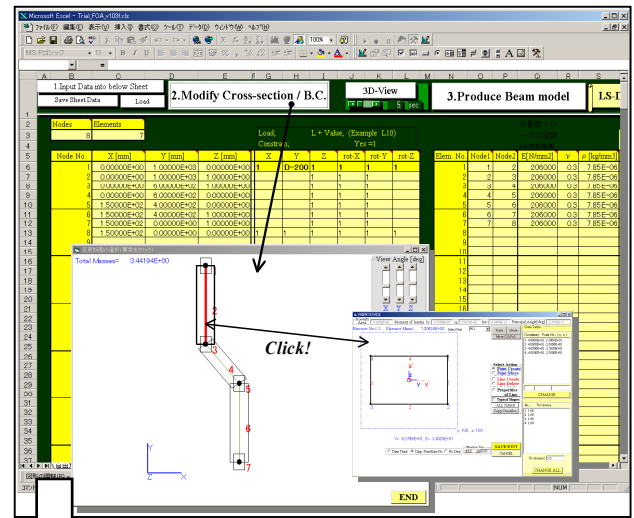
collapse range. The element behavior under uniaxial and biaxial bending presented using simple models where various effects can be easily traced. Kim and Wierzbicki [5] had investigated the crushing response of thin-walled prismatic column under combined loading of compression and bending to develop simplified crash-oriented design tools. The initial and subsequent failure loci-representing interaction between sectional force and moment were constructed from the numerical results. Also analytical solution of the same problem was derived. Takada and Abramowicz [6] had presented the object-oriented formulation of the finite element algorithm that encompasses traditional finite element, super element, experimental data, and codes of practice and rigid body mechanics in a single calculation environment. This formulation is implemented in software for dynamic crash simulation of an arbitrary 3D-frame structure discretized into superbeam elements and subjected to large dynamic crash loading.

In many cases, many structural members of the automotive body are subject to a combined compression-bending loading, and the cross-sectional shape is also arbitrary. Furthermore, considering that the engineering designers themselves perform these examinations in a conceptual design stage, it is desirable to complete a series of work on one notebook type personal computer with simple operation.

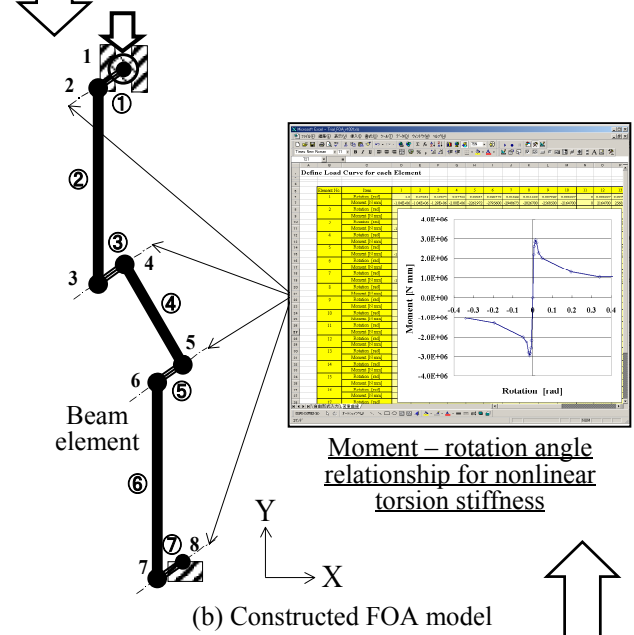
In this paper, the concept of FOA described above is applied to prediction of the collapse characteristic of the structure component of the body. First, cross-sectional shape is created by mouse operation, and the material characteristic is inputted in dialogue form. By the above operation, the FEA model by the shell element, which extended cross-sectional shape automatically, is created. Collapse analysis under loading conditions of combined axial force and bending moment is carried out to this easily created linear cantilever. Next, the finite element analysis model of structural member using a beam element is created. The collapse characteristic obtained at the previous step is given into a bending collapse part in a whole model. Then, the energy absorption characteristic etc. is easily predicted by carrying out collapse analysis of structural member.

FOA SYSTEM FOR CRASHWORTHINESS ANALYSIS

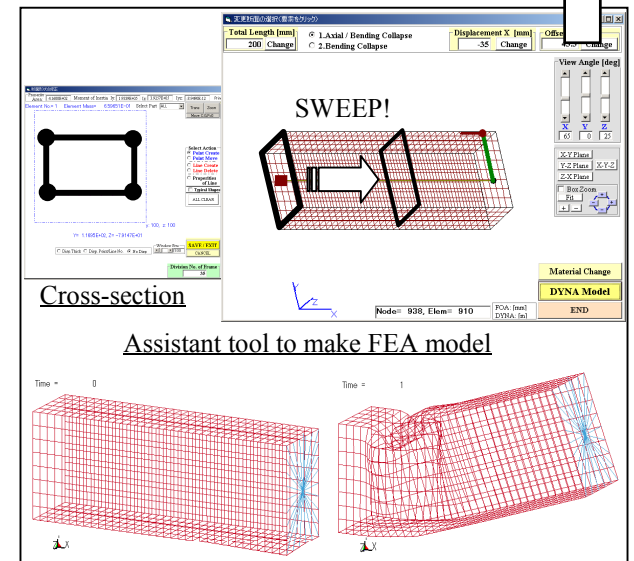
In FOA, by regarding easiness of understanding of the mechanical characteristic, beam elements and panel elements are fundamentally used. FOA system for this crashworthiness analysis uses beam element with nonlinear characteristics (Figure 1). In-house finite element analysis (FEA) software is used for this analysis. This software can be analyzed simultaneously in consideration of large deformation and vibration of structure. And this software is based on the beam theory, which updates the coordinates of structure for every time step, and calculates the dynamic response of structure by direct numerical integration. Moreover, this software can also treat a beam element with nonlinear stiffness.



(a) Excel sheet for FOA beam element



(b) Constructed FOA model



(c) Collapse analysis-using LS-DYNA for bending part

Figure 1. FOA system for crashworthiness analysis

The graphical interface constructed on Excel is prepared in order to make this FOA model (Figure 1(a)). Excel is equipped with the so-called Visual Basic for Application (VBA). Using this function, clicking actions lead to (1) write/read data in cells, (2) move to a different sheet, (3) calculate some schemes, (4) I/O with external files, and (5) start external programs. FEA analysis of the shell model using general-purpose transient dynamics finite element program LS-DYNA is carried out in order to obtain the collapse characteristic of the bending part (Figure 1(c)). The assistant tool is prepared so that the engineering designer may easily make this shell model. This collapse characteristic of the bending part can also be used by the results of the experiment. And these characteristics are inputted into the above FOA beam model (Figure 1(b)).

ASSISTANT TOOL FOR COLLAPSE CHARACTERISTIC OF BENDING PART

FEA model using shell element is automatically created by extending the cross-sectional shape. This model can be obtained only by creating the cross-sectional shape and inputting the material characteristic. After that, collapse analysis (quasi-static analysis by implicit approach) under the loading condition of combined axial force and bending moment of linear cantilever is carried out. The flow of procedure is shown in Figure 2. Procedure is summarized as follows:

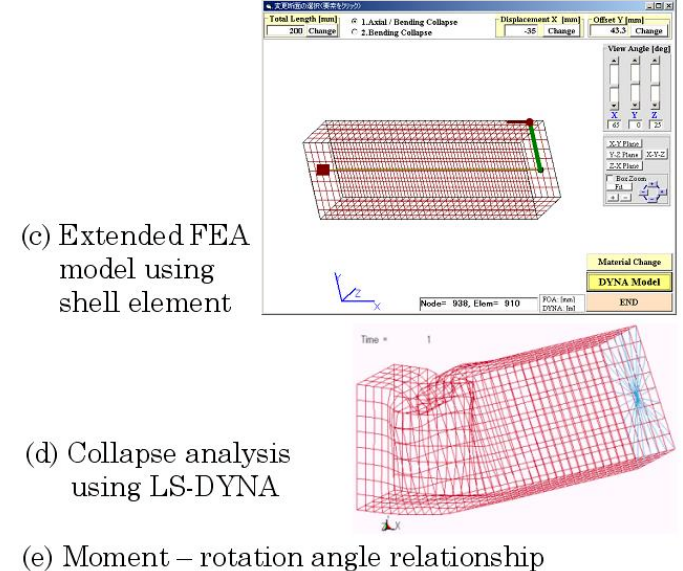
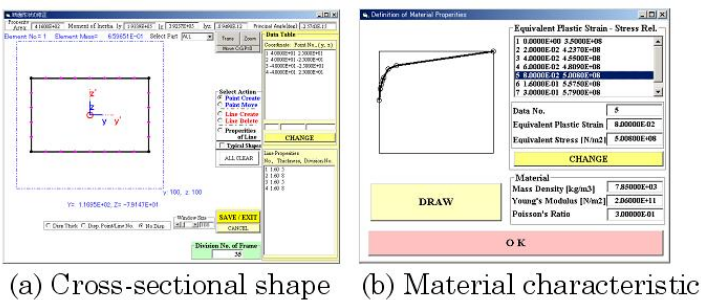


Figure 2. Flow of procedure to obtain collapse characteristic of bending part

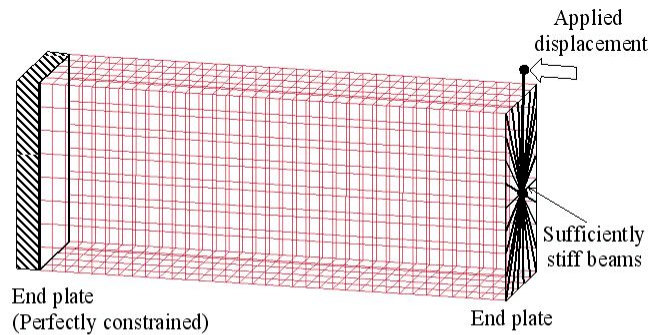
- Design of cross-sectional shape.
- Modification of the material characteristic.
- Construction of extended FEA model using the shell element.
- Collapse analysis using LS-DYNA.
- Post process of “ moment – rotation angle relationship”.

OPERATIONAL PROCEDURE

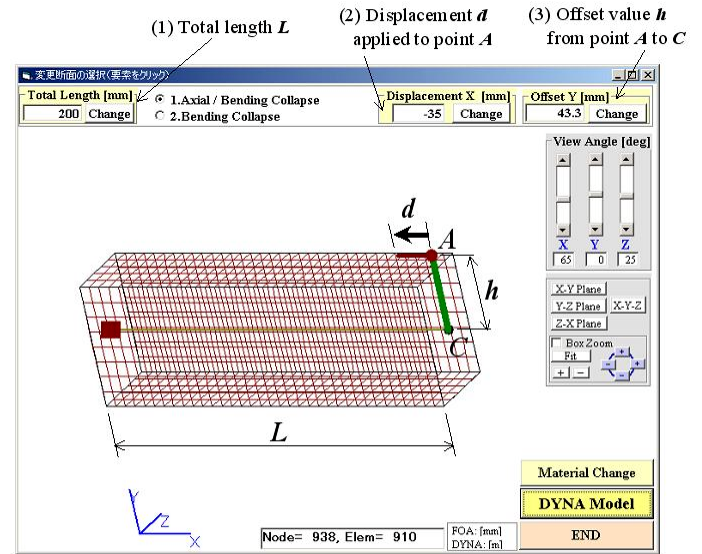
Here, the operational procedure of the assistant tool to obtain the collapse characteristic of bending part is explained.

Loading condition of collapse analysis is shown in Figure 3(a). A left end is perfectly constrained. The arbitrary displacement, which increases in linearly, is given to a right end. The end plate is represented by connecting all nodes of a right end cross section with a sufficiently stiff beam to the center node of a cross section. Furthermore, extending a sufficiently stiff beam from the central point of a cross section enables the input of offset value.

The main operation items in this main operation frame (Figure 3(b)) are summarized as follows:



(a) Loading condition of combined axial force and bending moment of cantilever



(b) Operation items of main frame

Figure 3. Main operation frame to obtain collapse characteristic of bending part

- (1) Total length L .
- (2) Arbitrary displacement d applied to an upper right side point A .
- (3) Offset value h from the central point C of cross section to an above-mentioned applied point A .

The axial collapse characteristic can also be obtained by setting the offset value h to 0. In addition, by clicking the "DYNA Model" button, the node number and element number of input data for LS-DYNA are displayed, and amount of a model can be checked.

Next, the creation procedure of cross-sectional shape is explained. If member is clicked at the main operation frame (Figure 3(b)), frame, which creates cross-sectional shape as shown in Figure 4, will appear. While we can create and modify the cross-sectional shape by mouse operation, morphing (another operation frame appears by click of the "Zoom" button) of this shape can also be performed. Furthermore, in order to create a FEA model, the number of division of the axial direction when extending cross-sectional shape can be changed.

Next operation is the input of the material characteristic. If a "Material Change" button is clicked at the main operation frame (Figure 3(b)), the input frame of the material characteristic shown in Figure 5 will appear. First, "Mass density", "Young's modulus", and a "Poisson's ratio" can be inputted with the "Material" frame at the lower right side. By the default, the iron characteristic is always given. Next, a check and correction of the relationship between equivalent plastic strain and an equivalent stress can be made. By clicking the "DRAW" button, this relationship can be displayed in a graph image (horizontal axis: equivalent plastic strain, vertical axis: equivalent stress). In the "Equivalent Plastic Strain – Stress Rel." frame at the upper right side, equivalent plastic strain and the equivalent stress which were clicked are inputted into a lower text box, and can be changed.

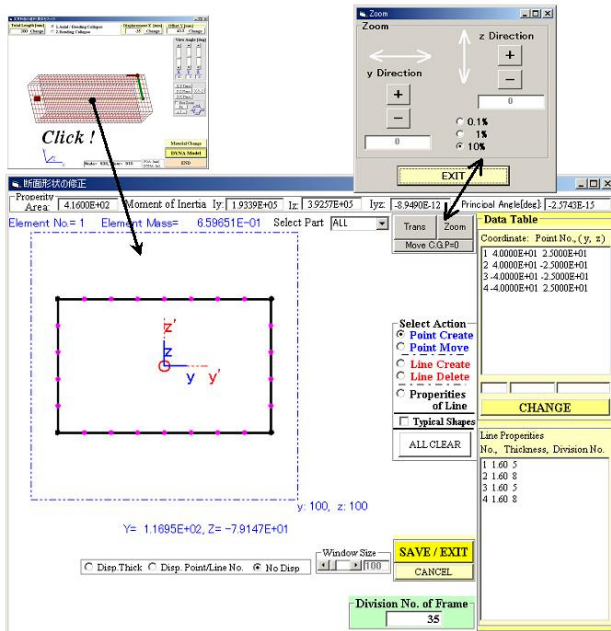


Figure 4. Sub frame to create cross-sectional shape

In addition, the generated moment M is estimated by the product of the reaction force F_x of displacement applied point, and the offset value ΔY from the center of the cross section of perfectly constrained side, as shown in Figure 6.

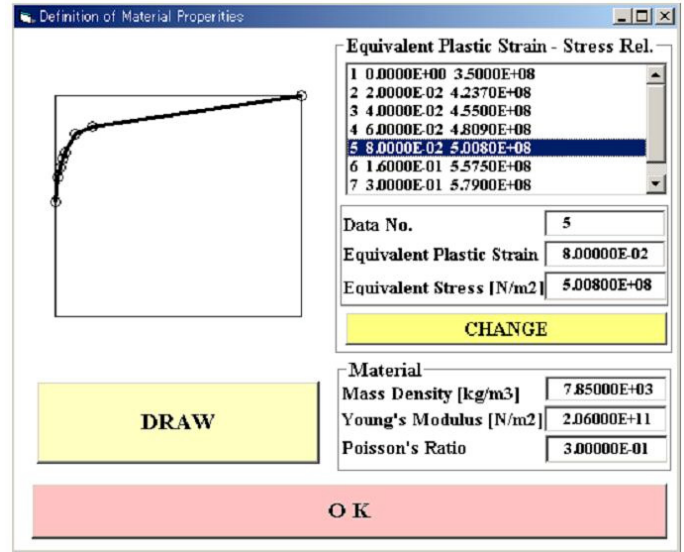


Figure 5. Sub frame to input material characteristic

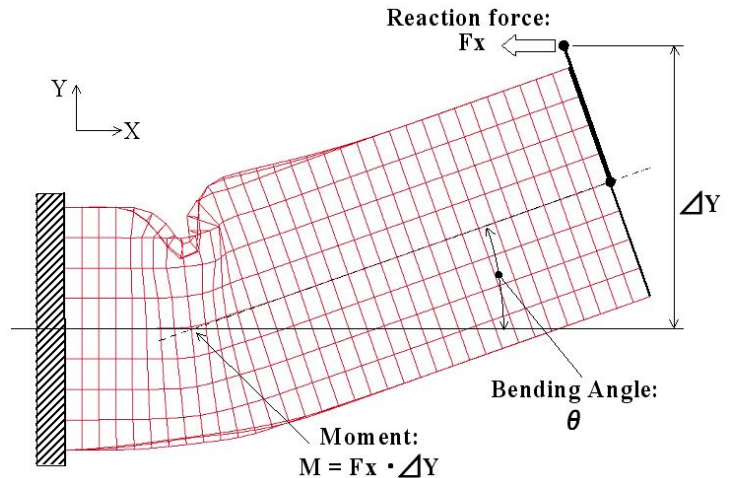


Figure 6. Relationship between applied moment M and deformed shape

COLLAPSE ANALYSIS METHOD OF STRUCTURAL MEMBER

In this stage, the finite element analysis model of structural member using beam element is created, and the collapse characteristic that obtained by previous step to bending part is given. And prediction of the energy absorption characteristic etc. is simply enabled by carrying out collapse analysis of structural member.

In usual case, LS-DYNA can be used for analysis solver for this like problem. "MAT_FORCE_LIMITED" material model is prepared in the LS-DYNA to realize the plastic hinge concept. This material model is available for the Belytschko resultant beam element. Plastic hinges form at the ends of the beam when the moment reaches the plastic moment. The moment versus rotation relationship is specified by the user in the form of a load curve and scale factor (Hallquist [7]).

But, in this paper, we also use the in-house finite element analysis software for the analysis of structural member to perform the basic study. This software can be analyzed simultaneously in consideration of large deformation and vibration of structure. And it is the finite element analysis software based on the beam theory, which updates the coordinates of structure for every time step, and calculates the dynamic response of structure by direct numerical integration (Ishiyama [8], Nishigaki [9] and Akasaki [10]). Moreover, this software can also treat a beam element with nonlinear torsion stiffness (Nishigaki [11]).

DESCRIPTION OF THE MOTION OF A FLEXIBLE STRUCTURE

To analyze the large deformation of a structure, we used an incremental finite element method and step by step time integration method. Namely, the coordinates of the nodes are modified at each incremental time step; thus, geometrical nonlinear characteristic is treated by stepwise linear approximation.

Figure 7(a) illustrates a beam which is an element of a three dimensional flexible structure. The position vector $\{r\}_i$ of the i -th node is defined by the global coordinates X, Y and Z,

$$\{r\}_i^T = \{X_i, Y_i, Z_i, \theta_{Xi}, \theta_{Yi}, \theta_{Zi}\} \quad (1)$$

The superscript T denotes the transpose of the matrix. The force vector $\{S\}_j$ of the j -th element is defined by the local coordinates x, y and z,

$$\{S\}_j^T = \{S_1, S_2, S_3, S_4, S_5, S_6\} \quad (2)$$

In Eqn (2), S_1 denotes axial force, S_2, S_3, S_5 and S_6 are bending moments and S_4 denotes the torsion moment. The displacement vector corresponding to the force vector is expressed as $\{s\}_j$, where s_1 denotes the axial displacement, s_2, s_3, s_5 and s_6 are angles of rotation and s_4 denotes the torsion angle. The relation between $\{s\}_j$ and $\{r\}_j$ is given in terms of the transformation matrix $[a]_j$,

$$\{\dot{s}\}_j = [a]_j \{\dot{r}\}_j \quad (3)$$

The superdot denotes a time differential. When the mass of an element is allocated to the nodes as a lumped mass, the equations of motion for the nodes are written

$$\sum_{j=1}^{Ne} ([M]_j \{\ddot{q}\}_j) = - \sum_{j=1}^{Ne} [a]_j^T \{S\}_j + \{R\} \quad (4)$$

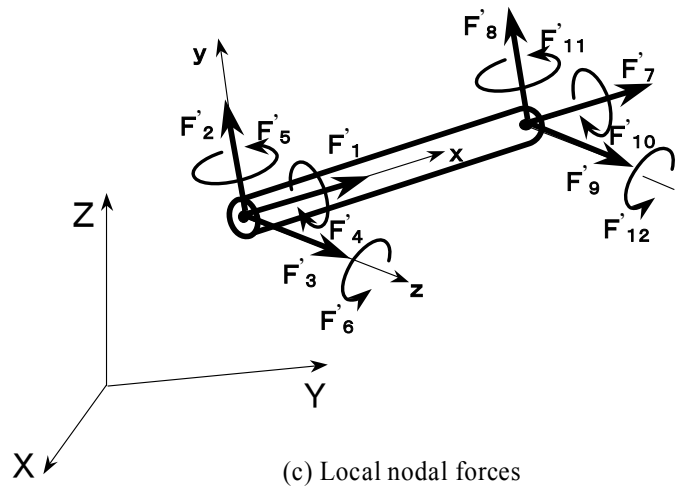
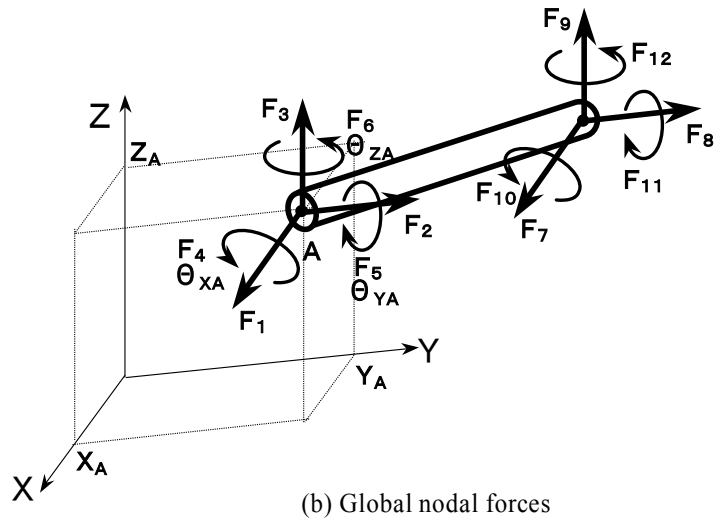
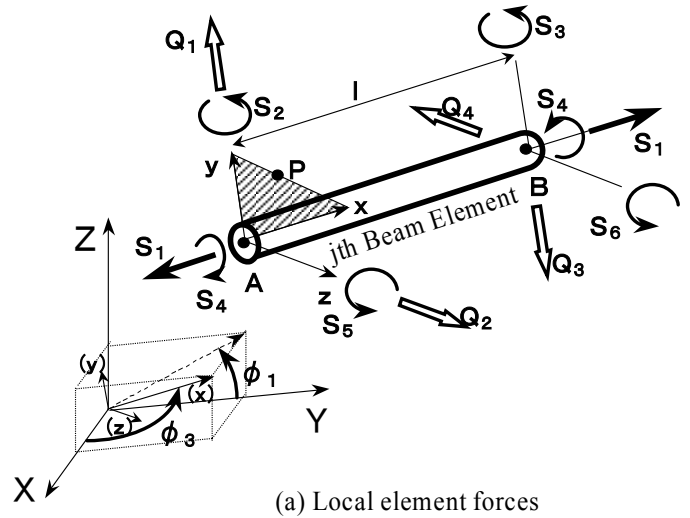


Figure 7. Local and global coordinates, force vector components of beam element

Where $[\mathbf{M}]$ is the mass matrix and $\{\mathbf{R}\}$ is the applied load vector. N_e is the number of elements, and $\{\mathbf{q}\}_j = \{\mathbf{r}\}_j$.

The coordinate transformation matrix $[\lambda]$ from the global to local coordinates can be written:

$$\{x, y, z\}^T = [\lambda] \{X, Y, Z\}^T \quad (5)$$

This matrix $[\lambda]$ is expressed in terms of the direction cosine (ξ, η, ζ) of the local x -axis to the global coordinates and a vector (X_{AP}, Y_{AP}, Z_{AP}) , which is located from nodal point A to point P . Where point P is used to determine the principal x - y surface of the cross-section of the element. Therefore, this point P is located on one of the principal surfaces and determines the local x - y plane with the local x -axis (Figure 7(a)),

$$[\lambda] = [\mathbf{B}] [\phi] \quad (6)$$

$$[\mathbf{B}] = \begin{bmatrix} 1 & 0 & 0 \\ 0 & \cos \beta & \sin \beta \\ 0 & -\sin \beta & \cos \beta \end{bmatrix}, \quad (7)$$

$$[\phi] = \begin{bmatrix} \phi_{11} & \phi_{12} & \phi_{13} \\ \phi_{21} & \phi_{22} & \phi_{23} \\ \phi_{31} & \phi_{32} & \phi_{33} \end{bmatrix} = \begin{bmatrix} \xi & \eta & \zeta \\ -\eta & \pm 1 \mp \frac{\eta^2}{1 \pm \xi} & \frac{\mp \eta \zeta}{1 \pm \xi} \\ \mp \zeta & \frac{-\eta \zeta}{1 \pm \xi} & 1 - \frac{\zeta^2}{1 \pm \xi} \end{bmatrix} \quad (8)$$

$$\left. \begin{aligned} \xi &= \cos \phi_3 \\ \eta &= \sin \phi_3 \cos \phi_1 \\ \zeta &= \sin \phi_3 \sin \phi_1 \end{aligned} \right\} \quad (9)$$

$$\left. \begin{aligned} \cos \beta &= y'_{AP} / \sqrt{y'^2_{AP} + z'^2_{AP}} \\ \sin \beta &= z'_{AP} / \sqrt{y'^2_{AP} + z'^2_{AP}} \end{aligned} \right\} \quad (10)$$

$$\left. \begin{aligned} y'_{AP} &= \phi_{21} X_{AP} + \phi_{22} Y_{AP} + \phi_{23} Z_{AP} \\ z'_{AP} &= \phi_{31} X_{AP} + \phi_{32} Y_{AP} + \phi_{33} Z_{AP} \end{aligned} \right\}$$

The sign convention in Eqn (8) is that if ξ is positive or zero, the upper signs are used and vice versa.

The transformation matrix $[\mathbf{a}]_j$ of the j -th element is derived by the following operations. The global nodal force vector $\{\mathbf{F}\}_j^T = \{F_1, F_2, F_3, \dots, F_{12}\}$ in Figure 7(b) constitutes a complete set of forces equal to the number of degrees of freedom assumed on the j -th element. From the principle of virtual work, we obtain:

$$\{\mathbf{F}\}_j^T \{\mathbf{q}\}_j = \{\mathbf{S}\}_j^T \{\mathbf{s}\}_j \quad (11)$$

Substituting Eqn (3) into Eqn (11), we obtain the relation between $\{\mathbf{F}\}_j$ and $\{\mathbf{S}\}_j$:

$$\{\mathbf{F}\}_j = [\mathbf{a}]_j^T \{\mathbf{S}\}_j \quad (12)$$

The relationship between $\{\mathbf{F}\}_j$ and the local nodal forces $\{\mathbf{F}'\}_j^T = \{F'_1, F'_2, F'_3, \dots, F'_{12}\}$ in Figure 7(c) is given by $\{\mathbf{F}\}_j = [\lambda]^T \{\mathbf{F}'\}_j$. Meek [12] has shown that the local element forces $\{\mathbf{S}\}_j^T = \{S_1, S_2, S_3, S_4, S_5, S_6\}$ are sufficient to define all the local nodal force vectors $\{\mathbf{F}'\}_j$. The transformation from $\{\mathbf{S}\}_j$ to $\{\mathbf{F}'\}_j$ is written

$$\{\mathbf{F}'\}_j = [\mathbf{L}]_j \{\mathbf{S}\}_j \quad (13)$$

$$[\mathbf{L}]_j = \begin{bmatrix} -1 & 0 & 0 & 0 & 0 & 0 \\ 0 & 0 & 0 & 0 & 1/l_j & 1/l_j \\ 0 & -1/l_j & -1/l_j & 0 & 0 & 0 \\ 0 & 0 & 0 & 1 & 0 & 0 \\ 0 & 1 & 0 & 0 & 0 & 0 \\ 0 & 0 & 0 & 0 & 1 & 0 \\ 1 & 0 & 0 & 0 & 0 & 0 \\ 0 & 0 & 0 & 0 & -1/l_j & -1/l_j \\ 0 & 1/l_j & 1/l_j & 0 & 0 & 0 \\ 0 & 0 & 0 & -1 & 0 & 0 \\ 0 & 0 & 1 & 0 & 0 & 0 \\ 0 & 0 & 0 & 0 & 0 & 1 \end{bmatrix}$$

Thus $[\mathbf{a}]_j^T$ is obtained using the coordinate transformation matrix $[\lambda]$ and the transformation matrix $[\mathbf{L}]_j$ which eliminates rigid-body motion in the local coordinates,

$$[\mathbf{a}]_j^T = [\lambda]^T [\mathbf{L}]_j = \begin{bmatrix} \lambda_j^T & \mathbf{0} & \mathbf{0} & \mathbf{0} \\ \mathbf{0} & \lambda_j^T & \mathbf{0} & \mathbf{0} \\ \mathbf{0} & \mathbf{0} & \lambda_j^T & \mathbf{0} \\ \mathbf{0} & \mathbf{0} & \mathbf{0} & \lambda_j^T \end{bmatrix} [\mathbf{L}]_j \quad (14)$$

Where l_j is the length of the j -th element.

The local element force vector $\{\mathbf{S}\}_j$ is related to the elemental deformations as follows. In order to damp the vibration of the beam elements, the visco-elastic Voigt model, which combines the viscous element with the elastic element in parallel, is introduced. The damping characteristics of the beam element are assumed to be proportional to the element stiffness matrix. The proportional factor is denoted by α . Thus, the constitutive equation for the beam element is described by

$$\{\dot{\mathbf{S}}\}_j = [\mathbf{k}]_j [[\mathbf{a}]_j (\{\mathbf{q}\}_j + \alpha \{\dot{\mathbf{q}}\}_j)] \quad (15)$$

The stiffness matrix of the beam element $[k]$ is given by:

$$[k]_j = \begin{bmatrix} \frac{EA}{l} & 0 & 0 & 0 & 0 & 0 \\ 0 & \frac{4EI_y}{l} & \frac{2EI_y}{l} & 0 & 0 & 0 \\ 0 & \frac{2EI_y}{l} & \frac{4EI_y}{l} & 0 & 0 & 0 \\ 0 & 0 & 0 & \frac{GJ}{l} & 0 & 0 \\ 0 & 0 & 0 & 0 & \frac{4EI_z}{l} & \frac{2EI_z}{l} \\ 0 & 0 & 0 & 0 & \frac{2EI_z}{l} & \frac{4EI_z}{l} \end{bmatrix} \quad (16)$$

Where E and G denote the modulus of elasticity and shear modulus of the beam, A , I and J are the cross sectional area, its moment of inertia and its polar moment, respectively.

Hence, by combining Eqn (3), (13), (14) and (15), the stiffness matrix $[k_s]_j$ is expressed in terms of local nodal force components $\{F\}_j$, as described by Meek[12]

$$[k_s]_j = [L]_j [k]_j [L]_j^T \quad (17)$$

We want to use a relatively large time step during direct integration in order to avoid unnecessary high frequency vibrations, so we should select the unconditionally stable scheme. Thus we use the Newmark β method ($\beta=1/4$), namely,

$$\{q_1\}_j = \{q_0\}_j + (h/2) (\{\dot{q}_0\}_j + \{\dot{q}_1\}_j) \quad (18)$$

$$\{S_1\}_j = \{S_0\}_j + (h/2) (\{\dot{S}_0\}_j + \{\dot{S}_1\}_j) \quad (19)$$

These equations are combined with Eqn (4) and (15), so simultaneous differential equations for $\{q\}_j$ and $\{S\}_j$ can be solved, where h is the time step and subscripts 0 and 1 indicate time t_0 and $t_1=t_0+h$, respectively.

The beam element used in FOA is the straight one. Therefore, in order to express the curved part, it is necessary to carry out polygonal line approximation. In this time, influence of the rigidity by curvature with the delicate surface of the wall in bending part, etc. are supposed to be disregarded.

In order to represent the nonlinear moment-rotation angle characteristic of bending part obtained by the previous step, the beam element that has nonlinear torsion stiffness is prepared. Since the stepwise linear approximation method is used, this nonlinear characteristic can be considered by giving tangent of the moment-rotation angle curve. It is also possible by setting up this element very short and joining in the direction of x , y , and z -axis together in series to give the

nonlinear moment-rotation angle characteristic over three dimensions to a joint part.

EXAMPLE

In order to verify the validity of this method, analysis for structural member shown in Figure 8 is carried out. First, (1) the moment-rotation angle characteristic is obtained with the easy operating tool to obtain the collapse characteristic of bending part. Next, (2) the finite element analysis model of structural member using a beam element is created. The collapse characteristic obtained at the previous step is given into a bending collapse part in a whole model. Then, the energy absorption characteristic etc. is easily predicted by carrying out collapse analysis of structural member. The collapse analysis result of the detailed shell element model using LS-DYNA is used for verification.

Cross-sectional shape of structural member is a rectangle (width: 80mm, height: 50mm and thickness: 1.6mm). Loading and boundary condition is shown in Figure 9. Structural member for analysis is connected with two sets by sufficiently stiff members. And these members are compressed in vertical direction. The material is iron. These values are shown in Figure 10.

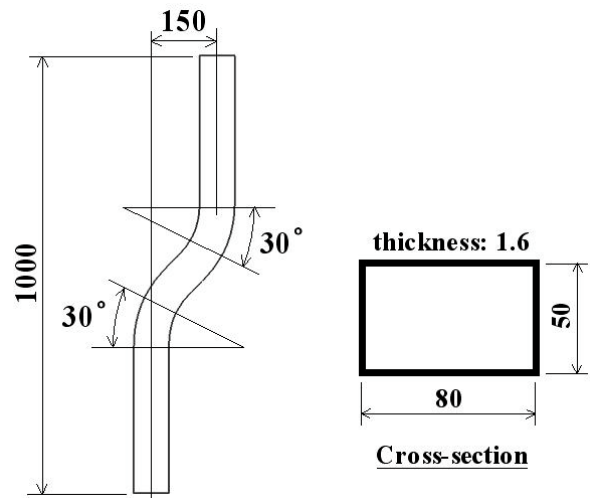


Figure 8. Dimensions of structural member for example

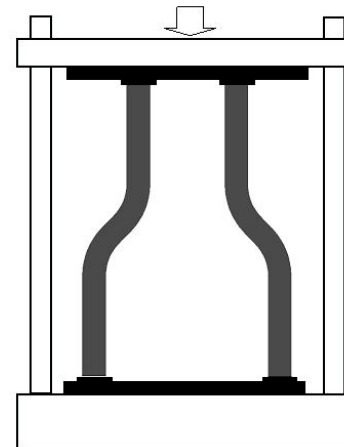


Figure 9. Loading and boundary condition for example

As a result of preliminary linear analysis using beam element according to the loading and the boundary condition shown in Figure 9, the value of the ratio of the moment and load of curved part was 43.3. Therefore, Offset value h in Figure 3(b) is set to 43.3mm. This time, total length L in Figure 3(b) is set to 200mm. The displacement d in Figure 3 is set to 35mm.

The deformation shape of the analysis result of this condition is shown in Figure 11. As shown in Figure 12, data processing of the moment-rotation angle characteristic obtained in this analysis is automatically carried out by Excel using a macro language. In addition, moment M is calculated as mentioned above relationship shown in Figure 6.

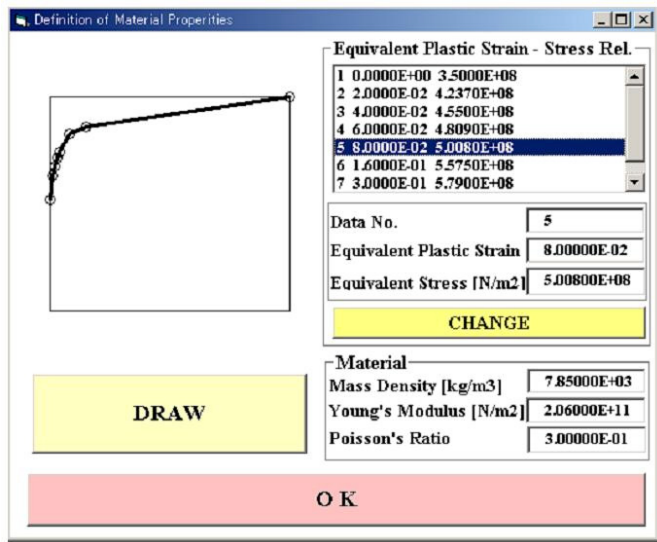


Figure 10. Material property (iron)

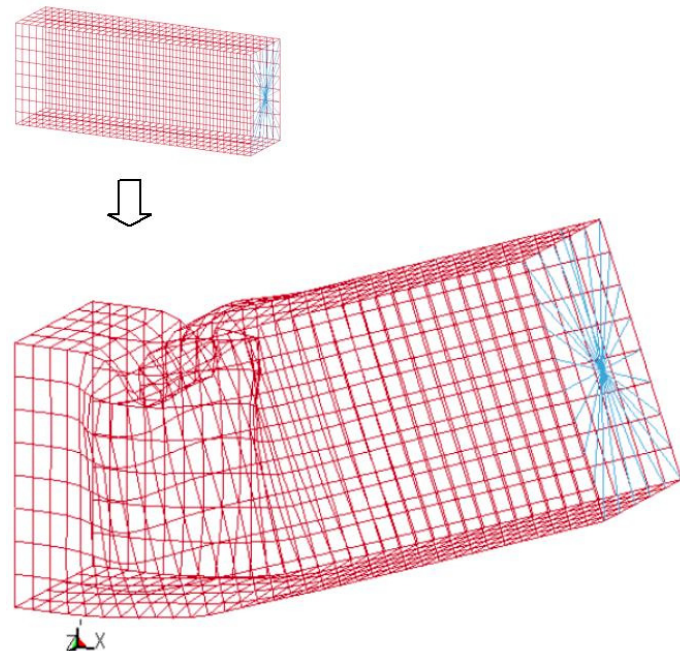


Figure 11. Deformation shape obtained by collapse analysis of cantilever using LS-DYNA

Collapse analysis of structural member is carried out using the FOA tool. First, the moment-rotation angle characteristic of bending part calculated above is inputted into the Excel sheet by reducing the redundant data (Figure 13). Next, in another Excel sheet (Figure 14), the FEA model using the beam element of structural member is created. Here, coordinates of each node and the constraint and loading conditions over each degrees of freedom are set as each cell of an Excel sheet. Furthermore, the beam model information except the cross-sectional characteristic is created by inputting the node number of the start and end point of each element. Cross-sectional shape can be easily modified by mouse operation in another frame which appear by clicking "Modify Cross-section / B.C." button.

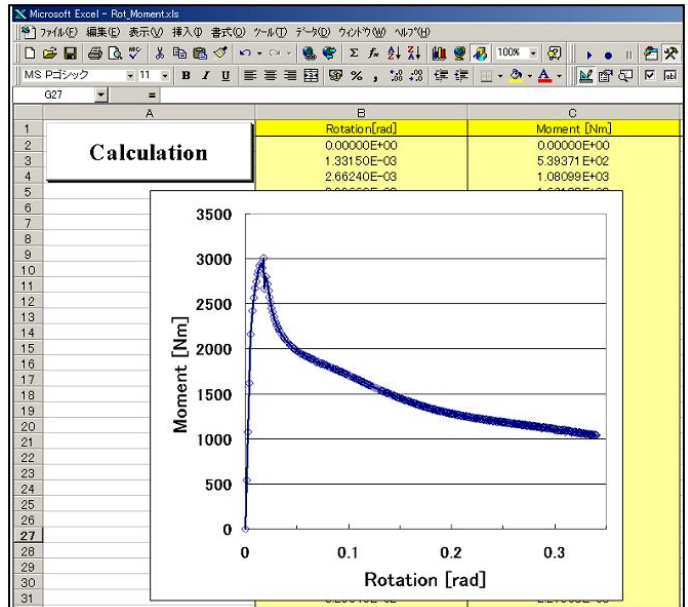


Figure 12. Moment-rotation angle characteristic automatically obtained by Excel using a macro language

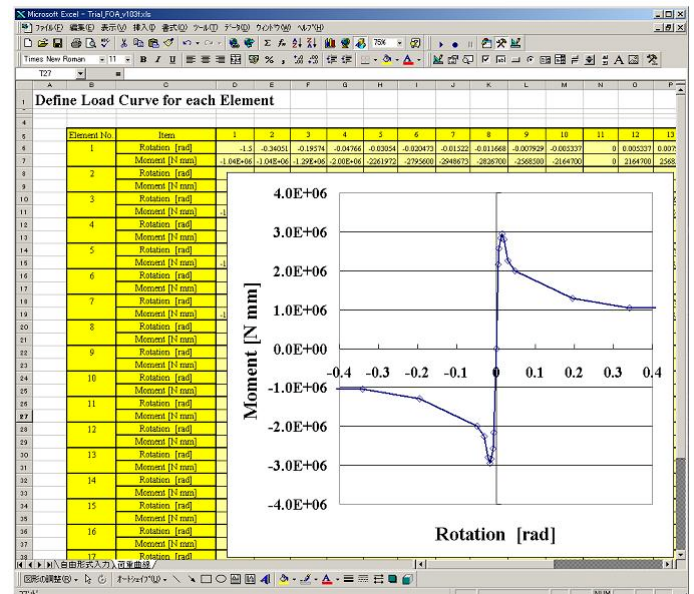


Figure 13. Moment-rotation angle characteristic inputted into Excel sheet by reducing redundant data

By the way, as for the beam element, which has the nonlinear torsion characteristic for expressing the moment-rotation angle characteristic of bending part, it is desirable for the length to be theoretically close to zero. The length of this beam element is set to 1mm in this paper.

The model created here is roughly shown in Figure 15. In this figure, element ①, ③, ⑤ and ⑦ are the beam element which have the nonlinear torsion characteristic with a length of 1mm, and remaining element ②, ④, and ⑥ are the usual beam element.

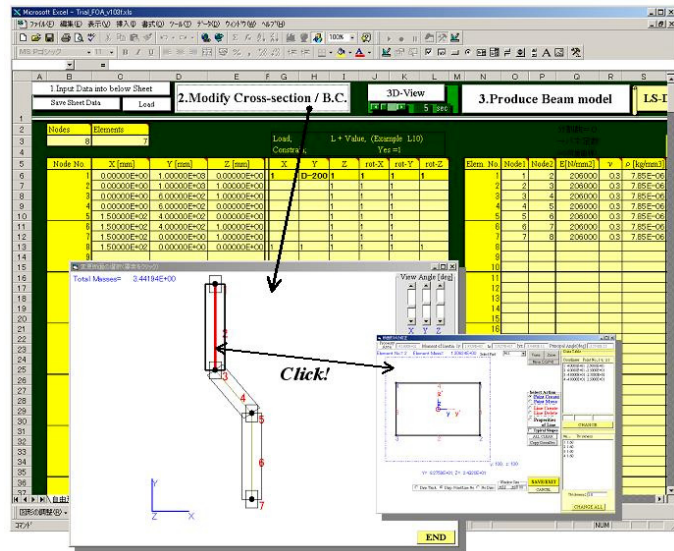


Figure 14. Excel sheet for FEA model using beam element of structural member

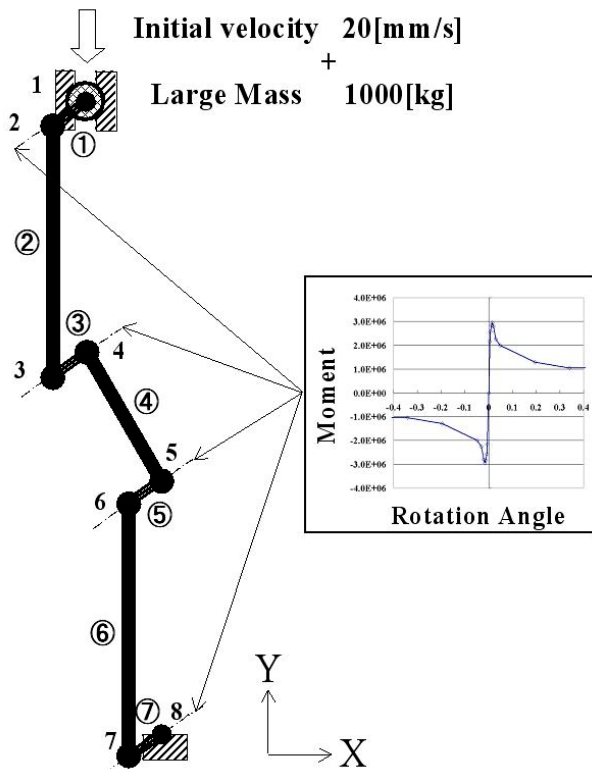


Figure 15. Illustration of FEA model for in-house software

Bottom node 8 is perfectly constrained (six degrees of freedom are constrained). Top node 1 is constrained about five degrees of freedom except the vertical direction (Y-axis direction). As for loading conditions, a quasi-static state is assumed. The mass of 1000kg is given to top node 1 as Large Mass, and initial velocity 20 [mm/sec] is given downward (opposite Y-axis direction). By the analysis to 10sec, final displacement is 200mm. In addition, since sufficiently large mass is given, the speed of node 1 is constant. Therefore, displacement is increasing in linearly. The input data of the in-house finite element analysis program based on beam theory is automatically created by mouse click in the "Produce Beam Model" button of the FOA tool shown in Figure 14. Moreover, this program can be performed automatically.

Figure 16 shows the detailed FEA model using the shell element created for verification. Type 16 in LS-DYNA, which is fully integrated formulation, is chosen as the shell element formulation. Number of through thickness integration points is set to 5. Type 24 in LS-DYNA, which is an elasto-plastic material with an arbitrary stress versus strain curve, is chosen as material type.

The deformation shapes obtained by these analyses are shown in Figure 17. In both analysis results, three hinges are created at bending part except a bottom end. Two results show that these deformed shapes are almost same.

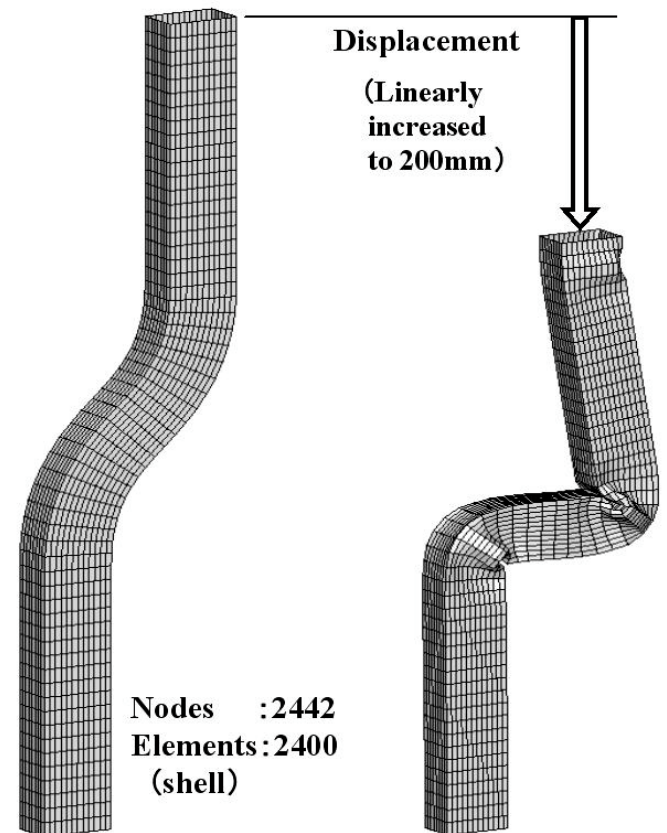


Figure 16. Detailed FEA model using shell element for verification

The relationship between the reaction force (the value of the vertical direction: F_y) and displacement (δY) of a moving point obtained by FOA and detailed FEA for verification are shown in Figure 18. By comparison with these results, it is verified that the result by simple FOA tool created for engineering designers can obtain the almost same result as LS-DYNA using the detailed shell element. Thereby, it is able to be shown that this method is effective and appropriate one.

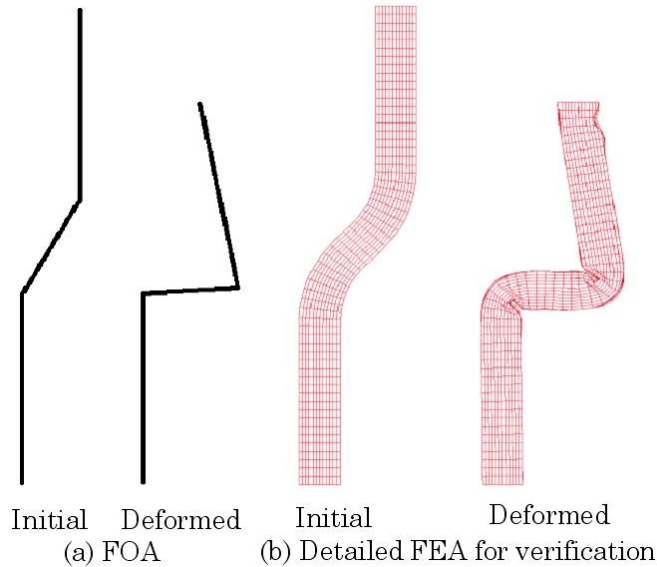


Figure 17. Deformed shapes obtained by FOA and detailed FEA for verification

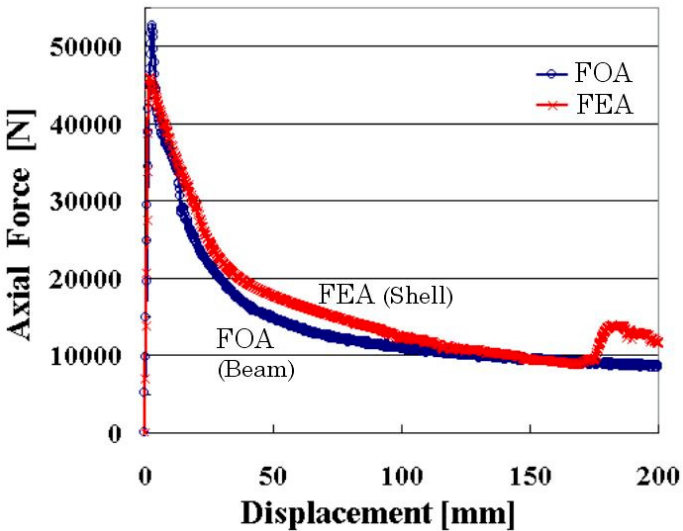


Figure 18. Relationship between reaction force (F_y) and displacement (δY) of moving point obtained by FOA (Beam) and detailed FEA (Shell) for verification

CONCLUSION

In this paper, we focus on the crashworthiness, and present the method to predict the collapse behavior of the frame member. This method is divided into two parts. Those are (1) collapse analysis under loading

conditions of combined axial force and bending moment to the cantilever, and (2) collapse analysis of structural member considering the previously obtained moment – rotation angle relationship using the beam element. In comparison with the results according to the detailed FEA model, effectiveness and validity of this method are presented.

REFERENCES

1. Nishigaki H., Nishiwaki S., Amago T. and Kikuchi N., 2000, "First Order Analysis for Automotive Body Structure Design", ASME DETC2000/DAC-14533.
2. Abramowicz W., 1981, "Simplified crushing analysis of thin-walled columns and beams", Eng. Trans, 29(1), pp. 5-26.
3. Kecman D., 1983, "Bending collapse of rectangular and square section tubes", Int. J. Mech. Sci., 25(9/10), 623-36.
4. Kecman D., Sadeghi M. and Vignjevic R., 1992, "The compound beam element with non-linear moment-rotation curves for the side impact and roof crush analysis using DYNA3D program", SAE paper no.921072.
5. Kim H-S. and Wierzbicki T., 2001, "Crush behavior of thin-walled prismatic columns under combined bending and compression", Comput. Struct. 79, pp. 1417-1432.
6. Takada K. and Abramowicz W., 2002, "Novel Formulation of the 3D Large Deformation Beam element for Dynamic Crash Analysis(in Japanese)", JSAE paper no.20025436.
7. Hallquist J. O., 1998, "LS-DYNA Theoretical Manual", Livermore Software Technology Corp.
8. Ishiyama S., Takagi J., Yamamoto K. and Nishimura T., 1988, "Impact response of thin-walled frame structures", Int. J. Impact Engng, Vol.7, No.2, pp. 197-212.
9. Nishigaki H. and Kawashima K., 1998, "Motion Control and Shape Optimization of a Suitlike Flexible Arm", Structural Optimization 15, pp. 163-171.
10. Akasaki F., Shimojima S., Nishigaki H. and Ishiyama S., 1992, "Large deformation analysis of flexible hose by dynamic finite element method", 25th ISATA Symposia, pp. 663-670.
11. Nishigaki H., MIKI K. and Ishiyama S., 1999, "Development of the Impact Response Analysis Program of the Pedestrian Dummy (in Japanese)", JSME 12th Computational Mechanics Conference Paper No.99-5, pp. 481-482.
12. Meek, J.L., 1971, "Matrix structural analysis", New York: McGraw-Hill.

CONTACT

The corresponding author of this paper is Hidekazu Nishigaki. He is now working at Toyota Central R&D Labs Inc. His e-mail address is e0793@mosk.tytlabs.co.jp

$$\left. \begin{aligned} b_{(1)} &= -b_{(7)} = EA/l \\ b_{(2)} &= -b_{(9)} = 12EI_z/l^3, \quad b_{(3)} = -b_{(12)} = 12EI_y/l^3 \\ b_{(4)} &= -b_{(14)} = GJ/l \\ b_{(5)} &= 4EI_y/l, \quad b_{(6)} = 4EI_z/l \\ b_{(8)} &= b_{(10)} = 6EI_z/l^2, \quad b_{(11)} = b_{(13)} = -6EI_y/l^2 \\ b_{(15)} &= 2EI_y/l, \quad b_{(16)} = 2EI_z/l \end{aligned} \right\} \quad (2)$$

$$\left. \begin{aligned} b_{(1)} &= \frac{F_{x(x=l)}}{u_{(x=l)}} = EAq \frac{\cos(ql)}{\sin(ql)} \\ b_{(7)} &= -\frac{F_{x(x=0)}}{u_{(x=0)}} = -EAq \frac{1}{\sin(ql)} \end{aligned} \right\} \quad (5)$$

Torsional vibration

The differential equation of torsional vibration has the same form as that of longitudinal vibration:

$$\frac{\partial^2 \theta}{\partial x^2} - p^2 \theta = \frac{M}{GJ} \quad \left(p = \frac{\omega}{c_t}, \quad c_t = \sqrt{G/\rho} \right) \quad (6)$$

where, G is shear modulus, J is torsional constant and c_t is propagation velocity of a torsional wave. Using the same operation of longitudinal vibration, the dynamic stiffness elements of torsional vibration are expressed as:

$$\left. \begin{aligned} b_{(4)} &= \frac{M_{x(x=l)}}{\theta_{x(x=l)}} = GJp \frac{\cos(pl)}{\sin(pl)} \\ b_{(14)} &= \frac{M_{x(x=0)}}{\theta_{x(x=0)}} = -GJp \frac{1}{\sin(pl)} \end{aligned} \right\} \quad (7)$$

Bending vibration

The bending vibration of a beam is expressed by the following differential equation:

$$\frac{\partial^4 v}{\partial x^4} - k_y^2 v = \frac{F}{EI_y} \quad \left(k_y^2 = \frac{\rho A}{EI_y} \omega^2 \right) \quad (8)$$

where, I_y is area moment of inertia in the y-direction. The general solution of this equation is:

$$v = C_1 \{ \cos(k_y x) + \cosh(k_y x) \} + C_2 \{ \cos(k_y x) - \cosh(k_y x) \} + C_3 \{ \sin(k_y x) + \sinh(k_y x) \} + C_4 \{ \sin(k_y x) - \sinh(k_y x) \} \quad (9)$$

We must consider the translational and rotational directions separately for bending because they are coupled with each other. The first case is a beam considered on one-side, with forced vertical displacement of the other side operating under constrained rotational displacement shown in Figure 2.

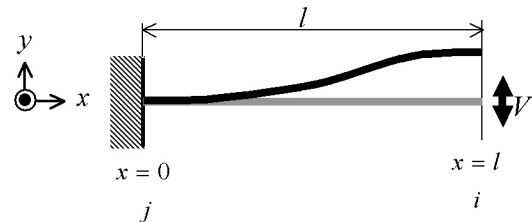


Fig. 2 Case of bending vibration of beam 1

However, for NV analysis, we must use a mass matrix and many finite elements to solve frequency response problems. We therefore use analytical dynamic solutions of Euler-Bernoulli beam theory, because these have high accuracy with few degrees of freedom. These formulations of the dynamic stiffness matrix are same as transfer matrix, however we solve these matrix same as FEM way. Furthermore, this analysis model can easily be changed from first order static analysis.

Longitudinal vibration

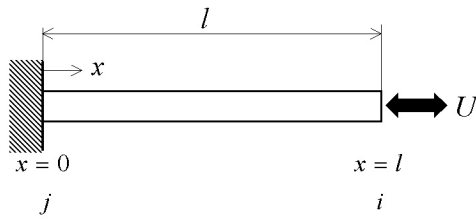


Fig. 1 Longitudinal vibration model of beam

The longitudinal vibration of a beam is expressed by the following differential equation:

$$\frac{\partial^2 u}{\partial x^2} - q^2 u = \frac{F}{EA} \quad \left(q = \frac{\omega}{c_l}, \quad c_l = \sqrt{E/\rho} \right) \quad (3)$$

where, E is Young's modulus, A is sectional area, ρ is density, ω is angular frequency and c_l is propagation velocity of a longitudinal wave. Considering the boundary conditions of $u=0$ at $x=0$ and $u=U$ at $x=l$ for the general solution $u=C_1 \cos(qx)+C_2 \sin(qx)$, the displacement u and force F are obtained as the following forms:

$$\left. \begin{aligned} u(x) &= U \frac{\sin(qx)}{\sin(ql)} \\ F_x(x) &= EA \frac{\partial u}{\partial x} = EA U q \frac{\cos(qx)}{\sin(ql)} \end{aligned} \right\} \quad (4)$$

so the elements of dynamic stiffness related to longitudinal vibration are expressed as:

Considering the boundary conditions of $v = 0, \partial v / \partial x = 0$ at $x=0$ and $v = V, \partial v / \partial x = 0$ at $x=l$, displacement v , shear force F_y and bending moment M_z are obtained by using constant C_2 — as follows:

$$\left. \begin{aligned} v(x) &= C_2 \left[\begin{aligned} &\left\{ \begin{aligned} &\cos(k_y x) - \cosh(k_y x) \\ &\frac{\sin(k_y l) + \sinh(k_y l)}{\cos(k_y l) - \cosh(k_y l)} \left\{ \sin(k_y x) - \sinh(k_y x) \right\} \end{aligned} \right\} \end{aligned} \right] \\ F_y(x) &= EI_y \frac{\partial^3 v}{\partial x^3} = C_2 EI_y k_y^3 \left[\begin{aligned} &\left\{ \begin{aligned} &\sin(k_y x) - \sinh(k_y x) \\ &-\frac{\sin(k_y l) + \sinh(k_y l)}{\cos(k_y l) - \cosh(k_y l)} \left\{ \cos(k_y x) + \cosh(k_y x) \right\} \end{aligned} \right\} \end{aligned} \right] \\ M_z(x) &= -EI_y \frac{\partial^2 v}{\partial x^2} = C_2 EI_y k_y^2 \left[\begin{aligned} &\left\{ \begin{aligned} &\cos(k_y x) + \cosh(k_y x) \\ &+\frac{\sin(k_y l) + \sinh(k_y l)}{\cos(k_y l) - \cosh(k_y l)} \left\{ \sin(k_y x) + \sinh(k_y x) \right\} \end{aligned} \right\} \end{aligned} \right] \end{aligned} \right\} \quad (10)$$

So in the case of operating vertical displacements, the elements of the dynamic stiffness matrix are expressed as:

$$\left. \begin{aligned} b_{(2)} &= -\frac{F_{y(x=l)}}{v_{(x=l)}} = EI_y k_y^3 \frac{\cos(k_y l) \sinh(k_y l) + \sin(k_y l) \cosh(k_y l)}{1 - \cos(k_y l) \cosh(k_y l)} \\ b_{(8)} &= \frac{M_{z(x=l)}}{v_{(x=l)}} = EI_y k_y^2 \frac{\sin(k_y l) \sinh(k_y l)}{1 - \cos(k_y l) \cosh(k_y l)} \\ b_{(9)} &= \frac{F_{y(x=0)}}{v_{(x=l)}} = -EI_y k_y^3 \frac{\sin(k_y l) + \sinh(k_y l)}{1 - \cos(k_y l) \cosh(k_y l)} \\ b_{(10)} &= -\frac{M_{z(x=0)}}{v_{(x=l)}} = -EI_y k_y^2 \frac{\cos(k_y l) - \cosh(k_y l)}{1 - \cos(k_y l) \cosh(k_y l)} \end{aligned} \right\} \quad (11)$$

The next case is that rotational displacement is operating under constrained vertical displacement as shown in Figure 3.

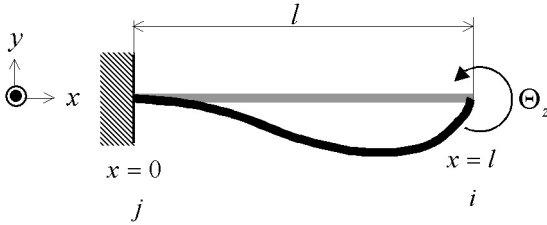


Fig. 3 Case of bending vibration of beam 2

The boundary conditions are $v = 0, \partial v / \partial x = 0$ at $x=0$ and $v = V, \partial v / \partial x = 0$ at $x=l$. Similarly, in the case of operating rotational displacements, the elements of the dynamic stiffness matrix are expressed as:

$$\left. \begin{aligned} b_{(6)} &= -\frac{M_{z(x=l)}}{\theta_{z(x=l)}} = -EI_y k_y \frac{\cos(k_y l) \sinh(k_y l) - \sin(k_y l) \cosh(k_y l)}{1 - \cos(k_y l) \cosh(k_y l)} \\ b_{(16)} &= \frac{M_{z(x=0)}}{\theta_{z(x=l)}} = -EI_y k_y \frac{\sin(k_y l) - \sinh(k_y l)}{1 - \cos(k_y l) \cosh(k_y l)} \end{aligned} \right\} \quad (12)$$

In the case of bending in the z-direction, the relation of direction between translation and rotation is different

from the case of bending in the y-direction shown in Figure 4. Therefore, some positive and negative signs are changed from the case of y-direction bending, and the elements of dynamic stiffness of bending in the z-direction are expressed as:

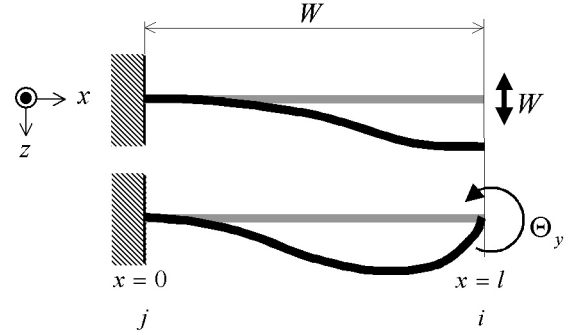


Fig. 4 Bending in z-direction

$$\left. \begin{aligned} b_{(3)} &= -\frac{F_{z(x=l)}}{w_{(x=l)}} = EI_z k_z^3 \frac{\cos(k_z l) \sinh(k_z l) + \sin(k_z l) \cosh(k_z l)}{1 - \cos(k_z l) \cosh(k_z l)} \\ b_{(11)} &= -\frac{M_{y(x=l)}}{w_{(x=l)}} = -EI_z k_z^2 \frac{\sin(k_z l) \sinh(k_z l)}{1 - \cos(k_z l) \cosh(k_z l)} \\ b_{(12)} &= \frac{F_{z(x=0)}}{w_{(x=l)}} = -EI_z k_z^3 \frac{\sin(k_z l) + \sinh(k_z l)}{1 - \cos(k_z l) \cosh(k_z l)} \\ b_{(13)} &= \frac{M_{y(x=0)}}{w_{(x=l)}} = EI_z k_z^2 \frac{\cos(k_z l) - \cosh(k_z l)}{1 - \cos(k_z l) \cosh(k_z l)} \\ b_{(5)} &= -\frac{M_{y(x=l)}}{\theta_{y(x=l)}} = -EI_z k_z \frac{\cos(k_z l) \sinh(k_z l) - \sin(k_z l) \cosh(k_z l)}{1 - \cos(k_z l) \cosh(k_z l)} \\ b_{(15)} &= \frac{M_{y(x=0)}}{\theta_{y(x=l)}} = -EI_z k_z \frac{\sin(k_z l) - \sinh(k_z l)}{1 - \cos(k_z l) \cosh(k_z l)} \end{aligned} \right\} \quad (13)$$

The angular frequency ω is included in its implicit form, and so normal eigensystem analysis cannot be used in these formulations. Instead, we use the determinant search method for eigenfrequency analysis. Although this method involves iterative calculation, it should not be a problem because this model has few degrees of freedom.

Note that the limit values of dynamic stiffness elements converge at the static values shown in Equation (1) as the values of angular frequency ω equal to 0.

VIBRATION POWER FLOW ANALYSIS

In order to verify the relation between vibration behavior and its reduction, we performed vibration power flow analysis, using the vibration intensity (VI) method proposed by Noiseux [2] and Pavic [3]. The fundamental theory of VI is expressed as a time-averaged value using velocity V and inner force F :

$$VI(\omega) = \frac{1}{T} \int_T (F(\omega, t) \cdot V(\omega, t)) dt \quad (14)$$

where, T is cyclic time. Many studies have examined VI for the bending vibration of a thin plate, because noise is mainly generated from bending vibration and it is difficult to accurately measure in-plane vibration. However, overall stiffness depends on local in-plane stiffness for a general structure like an automotive body, so we must consider in-plane vibration in order to verify and control the overall vibration energy. For the detailed formulation expressed by Equation (14), we separate element forces and moments. In Equation (14), F_z is vertical force, F_x is axial force, M_y is bending moment and M_x is torsional torque.

$$VI(\omega) = \frac{1}{T} \int_T \left(F_z \cdot \frac{\partial w}{\partial t} + M_y \cdot \frac{\partial \theta_y}{\partial t} + F_x \cdot \frac{\partial u}{\partial t} + M_x \cdot \frac{\partial \theta_x}{\partial t} \right) dt \quad (15)$$

In steady vibration, time-averaged power shows dissipation due to damping or outer forces, because the time-averaged conservative energy (kinetic and potential energy) is 0. So in this study we calculate the power flow for each phase without time averaging and verify the propagation of vibration energy between kinetic and potential energy as follows:

$$VI(\omega, t) = \frac{1}{2} \left(F_z \cdot \frac{\partial w}{\partial t} + M_y \cdot \frac{\partial \theta_y}{\partial t} + F_x \cdot \frac{\partial u}{\partial t} + M_x \cdot \frac{\partial \theta_x}{\partial t} \right) \sin(2\omega t) \quad (16)$$

In general, VI is expressed as a power flow vector. However, VI must be a scalar value because it is obtained by a vector product. That is, VI is the vector in temporary coordinates, but its value has no objectivity about rotation of axis. VI therefore means power flow in and out from neighboring domains, and so is the integration function of conservative power on the boundary between neighboring domains.

For example, we study the relation between conservative energy and VI for longitudinal and bending vibration of the beam. First, we study longitudinal vibration of the beam shown in Figure 5.

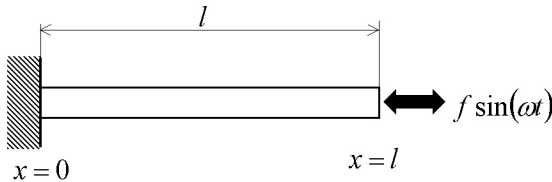


Fig. 5 Forced longitudinal vibration of beam

When outer force $F=f\sin(\omega t) \cdot \delta(x-l)$ is defined by the differential Equation (3), the following vibration response is obtained.

$$\begin{cases} u = \frac{f}{EAk \cos(ql)} \sin(qx) \sin(\omega t) \\ \frac{\partial u}{\partial x} = \frac{f}{EA \cos(ql)} \cos(qx) \sin(\omega t) \end{cases} \quad (17)$$

So the value of VI is formulated as:

$$VI = EA \frac{\partial u}{\partial x} \frac{\partial u}{\partial t} = \frac{\omega f^2}{4EAq \cos^2(ql)} \sin(2qx) \sin(2\omega t) \quad (18)$$

The strain energy U of this beam is expressed as:

$$U = \frac{1}{2} EA \left(\frac{\partial u}{\partial x} \right)^2 = \frac{f^2 \sin^2(\omega t)}{4EA \cos^2(ql)} \{1 - \cos(2qx)\} \quad (19)$$

and the kinetic energy T is expressed as following form.

$$T = \frac{1}{2} \rho A \left(\frac{\partial u}{\partial t} \right)^2 = \frac{f^2 \cos^2(\omega t)}{4EA \cos^2(ql)} \{1 + \sin(2qx)\} \quad (20)$$

The conservative energy W , which is the sum of U and T , is:

$$W = \frac{f^2}{8EA \cos^2(ql)} \{1 - \cos(2qx) \cos(2\omega t)\} \quad (21)$$

The integration function of conservative power (differential between W and time) is obtained as:

$$\int \frac{\partial W}{\partial t} dx = \frac{\omega f^2}{8EAq \cos^2(ql)} \sin(2qx) \sin(2\omega t) \quad (22)$$

Consequently, Equation (18) is proportional to Equation (22). The same formulation is obtained for torsional vibration.

Similarly, we study bending vibration of the beam shown in Figure 6. When outer force $F=f\sin(\omega t) \cdot \delta(x-l)$ is defined by the differential Equation (8), the following vibration response is obtained:

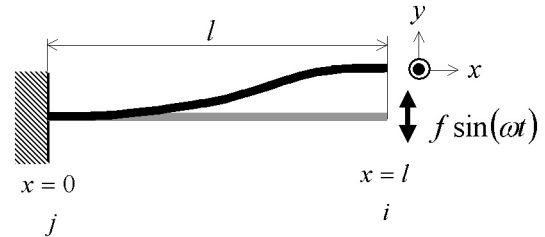


Fig. 6 Forced bending vibration of beam

$$\begin{cases} w = \frac{f \sin(\omega t)}{2EI k^3 \{1 + \cos(kl) \cosh(kl)\}} \left[\begin{aligned} & \{\sin(kl) + \sinh(kl)\} \{\cos(kx) - \cosh(kx)\} \\ & - \{\cos(kl) + \cosh(kl)\} \{\sin(kx) - \sinh(kx)\} \end{aligned} \right] \\ \frac{\partial w}{\partial x} = \frac{-f \sin(\omega t)}{2EI k^2 \{1 + \cos(kl) \cosh(kl)\}} \left[\begin{aligned} & \{\sin(kl) + \sinh(kl)\} \{\sin(kx) + \sinh(kx)\} \\ & + \{\cos(kl) + \cosh(kl)\} \{\cos(kx) - \cosh(kx)\} \end{aligned} \right] \\ \frac{\partial^2 w}{\partial x^2} = \frac{-f \sin(\omega t)}{2EI k \{1 + \cos(kl) \cosh(kl)\}} \left[\begin{aligned} & \{\sin(kl) + \sinh(kl)\} \{\cos(kx) + \cosh(kx)\} \\ & - \{\cos(kl) + \cosh(kl)\} \{\sin(kx) + \sinh(kx)\} \end{aligned} \right] \\ \frac{\partial^3 w}{\partial x^3} = \frac{f \sin(\omega t)}{2EI \{1 + \cos(kl) \cosh(kl)\}} \left[\begin{aligned} & \{\sin(kl) + \sinh(kl)\} \{\sin(kx) - \sinh(kx)\} \\ & + \{\cos(kl) + \cosh(kl)\} \{\cos(kx) + \cosh(kx)\} \end{aligned} \right] \end{cases} \quad (23)$$

The bending vibration of beam VI and the integration function of conservative power become the same formulations, operating in the same way as longitudinal vibration, as given by:

$$\begin{aligned} VI &= EI \left(\frac{\partial^2 w}{\partial x^2} \cdot \frac{\partial^2 w}{\partial x \partial t} - \frac{\partial^3 w}{\partial x^3} \cdot \frac{\partial w}{\partial t} \right) \\ &= \frac{\omega f^2 \sin(2\omega t)}{4EI k^3 \{1 + \cos(kl) \cosh(kl)\}^2} \\ &\times \left[\begin{aligned} & \{\sin(kl) + \sinh(kl)\}^2 \{\cos(kx) \sinh(kx) + \sin(kx) \cosh(kx)\} \\ & + \{\cos(kl) + \cosh(kl)\}^2 \{\cos(kx) \sinh(kx) - \sin(kx) \cosh(kx)\} \\ & - 2\{\sin(kl) + \sinh(kl)\} \{\cos(kl) + \cosh(kl)\} \sin(kx) \sinh(kx) \end{aligned} \right] \quad (24) \end{aligned}$$

$$\begin{aligned} \int \frac{\partial W}{\partial t} dx &= \frac{\omega f^2 \sin(2\omega t)}{4EI k^3 \{1 + \cos(kl) \cosh(kl)\}^2} \\ &\times \left[\begin{aligned} & \{\sin(kl) + \sinh(kl)\}^2 \{\cos(kx) \sinh(kx) + \sin(kx) \cosh(kx)\} \\ & + \{\cos(kl) + \cosh(kl)\}^2 \{\cos(kx) \sinh(kx) - \sin(kx) \cosh(kx)\} \\ & - 2\{\sin(kl) + \sinh(kl)\} \{\cos(kl) + \cosh(kl)\} \sin(kx) \sinh(kx) \end{aligned} \right] \quad (25) \end{aligned}$$

APPLICATION

As shown above, FOA for NV analysis can be used for the conceptual design of automotive substructures. We chose a simple front subframe model for its application. Of course, the main function of the subframe is to reinforce the body structure. Another function of the subframe is to cut off engine vibration to the main body, and so the subframe is sometimes mounted on rubber insulators on the main body frame. However, these insulators degrade the main function of the subframe. Thus, we must design the subframe cross-section, layout of beams and location of mounting positions at the conceptual design phase in order to cut off engine vibration.

We try to apply this analysis to a simple subframe model, and verify the effect of FOA for NV. The simple front subframe model is shown in Figure 7. It is mounted on the main frame of the automotive body and mounting engine by bushings. Generally, the elastic resonance frequency range of an engine is 300 – 500 Hz. In this study, we assume that the engine resonance frequency is 400Hz, and our task is to reduce this vibration to the main body at the conceptual design phase by examining the layout of beams and the location of mounting positions for this subframe.

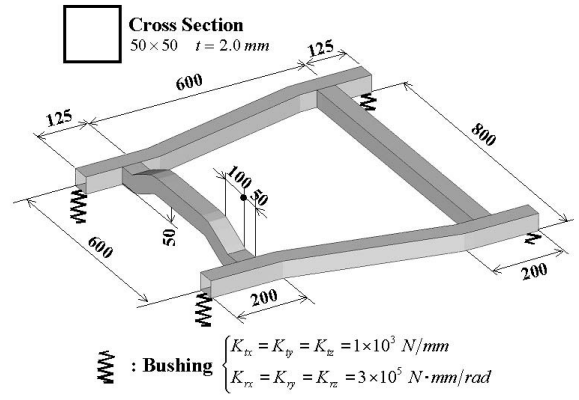


Fig. 7 Simple subframe model

EIGENFREQUENCY ANALYSIS

First, we calculate the eigenfrequency of this subframe, because the key point is to separate the resonance frequency of the engine and that of the subframe in order not to increase the influence of engine resonance. In this study, we compare the results of FOA to those of the FEM shell model to check the accuracy of FOA shown in Figure 8.

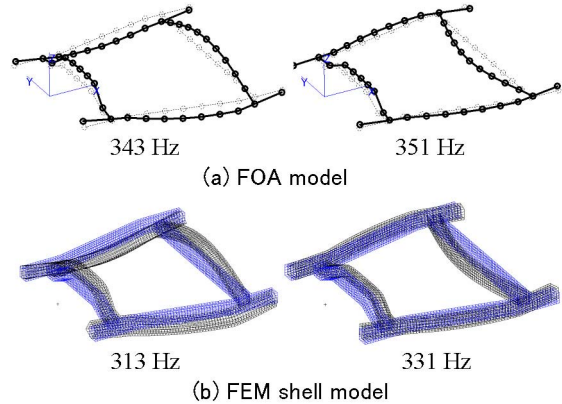


Fig. 8 Results of eigenfrequency analysis

From this result only two eigenvalues exist between the 300 – 500Hz frequency range, so at least this subframe dose not propagate and increase engine vibration to the main body.

The joint stiffness of this FOA model is taken from a database [4]. Eigenmodes show good consistency for the FOA and FEM shell model, however, eigenvalues are about 10% different using this database. More accurate joint modeling of FOA for NV is required in the future.

STUDY OF VIBRATION REDUCTION

Next, the frequency response is calculated assuming that the engine resonance vibration is 400Hz as shown in Figure 9. We observe the vibration response at connecting points by bushings to the main body frame.

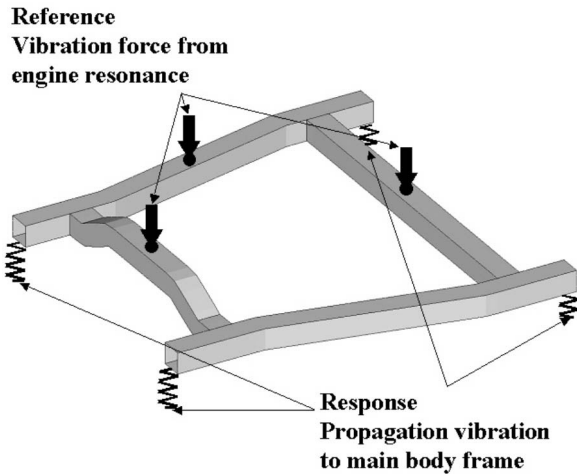


Fig. 9 Reference and response of subframe

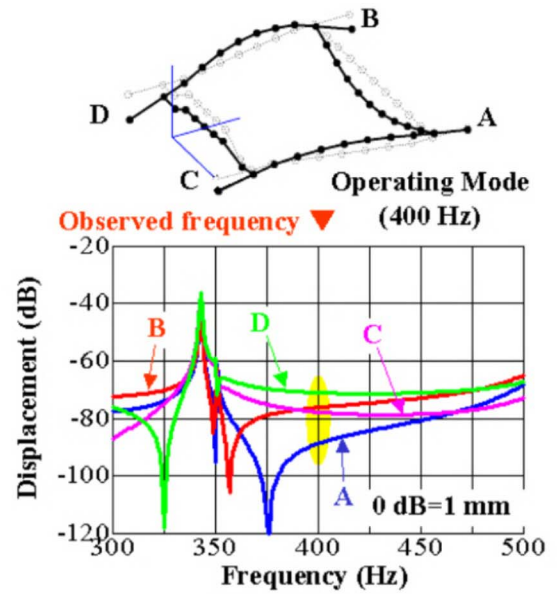
Engine resonance forces at three supported points are assumed to be unit forces with the same phase as each other, and the responses of vertical displacement are calculated at the connecting points to the main body. The results are shown in Figure 10 in comparison with the FEM shell model.

These results show that the responses of the four points have good consistency with the FOA and FEM shell models.

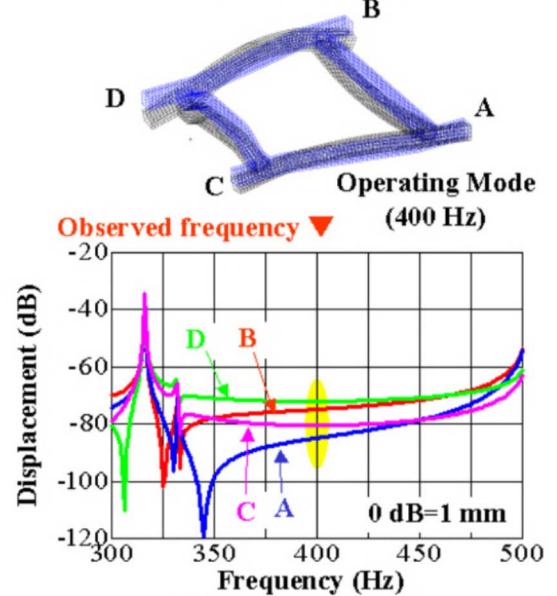
We must decrease the displacement at these points in order to reduce the propagation of vibration from the engine to the main body. We therefore tried to improve the beam layout and mounting positions of the engine as shown in Figure 11.

First, the location of the cross-frame is moved by 25 mm to control the first bending mode of the side-frames. Next, the mounting positions of the engine are changed at the connecting points of the cross-frames and side-frames, because these points are the nodes of this operating mode.

Using the modified subframe model shown in Figure 11, the frequency responses at observed points connecting to the main body are calculated as shown in Figure 12. From these results, the displacements of all observed points are reduced by about 10 dB at the target frequency of 400 Hz. The same reducing effects were also obtained for both the FOA model and FEM shell model.



(a) FOA model



(b) FEM shell model

Fig. 10 Frequency response of initial model

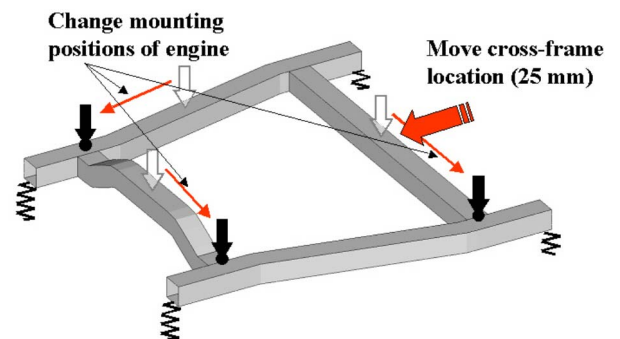


Fig. 11 Modified simple subframe model

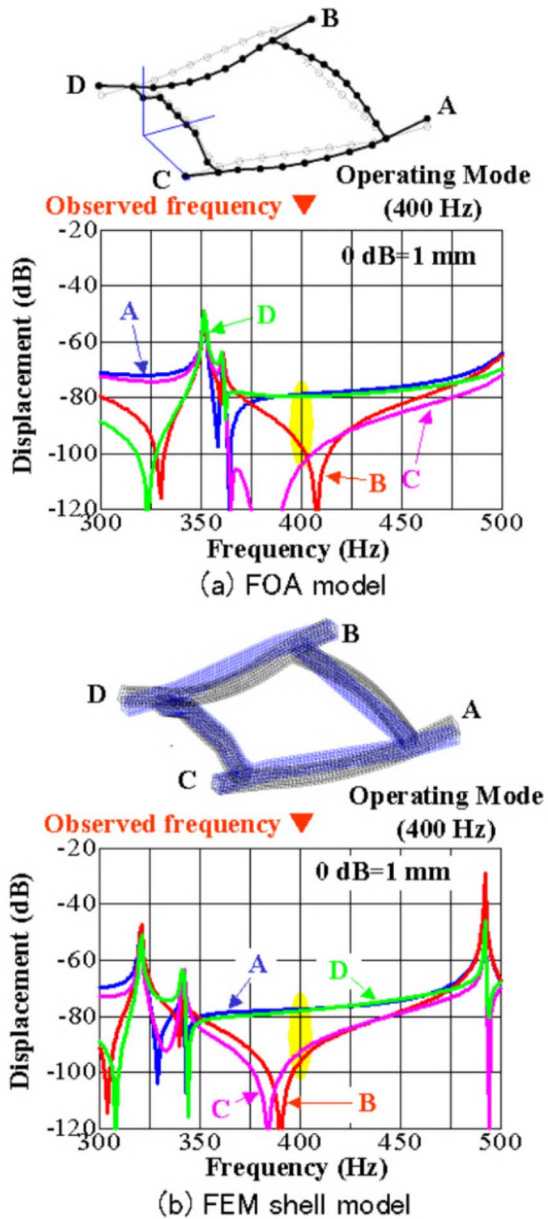


Fig. 12 Frequency response of modified model

VERIFICATION BY POWER FLOW ANALYSIS

When a general structure is divided into substructures, vibration propagates as displacement or strain, each of which is proportional to kinetic energy or strain energy. It may thus be useful to investigate the vibration power flow in order to reduce vibration by cutting off vibration energy to neighboring substructures. In the above study, the subframe vibration at connecting points of the main body was reduced, showing that power flow analysis is a useful way to learn about vibration reduction.

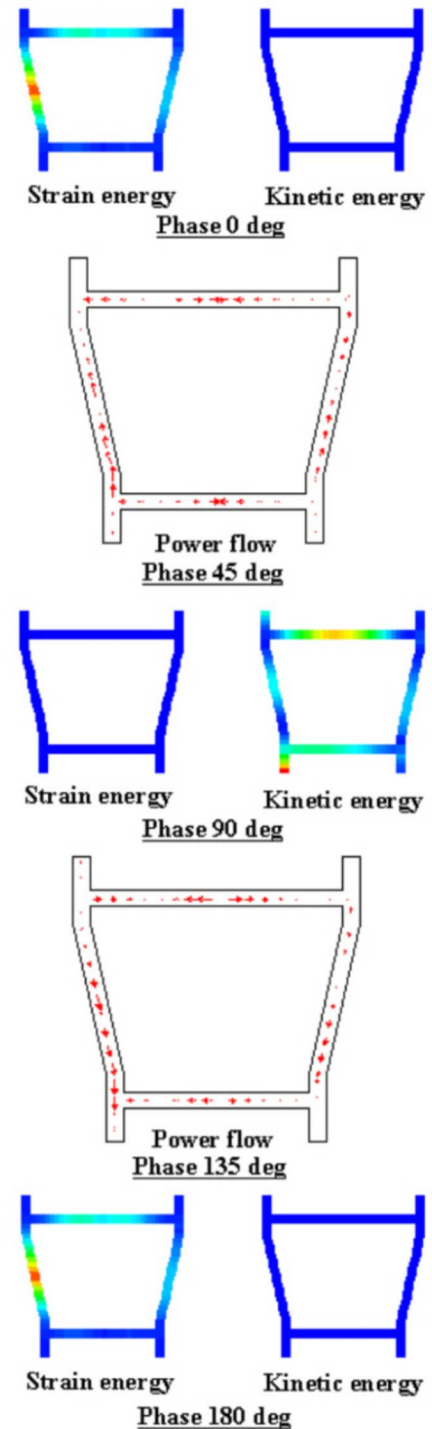


Fig. 13 Energy distribution and power flow of subframe (Initial model: 400 Hz)

The distribution of strain energy, kinetic energy and vibration power flow are calculated by using the equations given in the above sections. We apply this analysis to each subframe model at 400 Hz. We show three phases of conservative energy distribution: the first phase is maximum strain energy at 0 degree, the next is maximum kinetic energy at 90 degrees, and the last is

maximum strain energy again at 180 degrees. The power flow shows middle phases of energy distributions, which are 45 degrees and 135 degrees. Figure 13 shows the case of the initial subframe model, and Figure 14 shows that of the modified model.

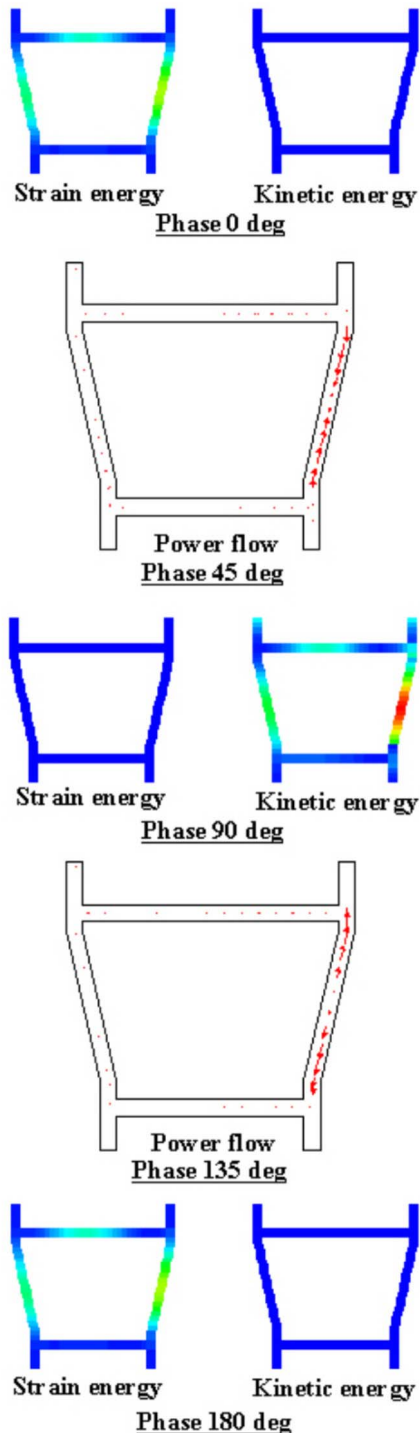


Fig. 14 Energy distribution and power flow of subframe (Modified model: 400 Hz)

From Figure 13 and 14, modifying the beam layout and forced points from engine vibration reduces the maximum kinetic energy distribution around connecting points to the main body. In the power flow of the initial model, oscillating strain energy on the left-side frame is propagated to the lower connecting point as kinetic energy. However, in the modified model, there is almost no energy propagation at cross frames or left-side frame, and there is only an exchange of strain energy for kinetic energy at the right-side frame. It is thus verified that power flow to the main body is cut off as a result of this modification.

CONCLUSION

In this study, we proposed FOA for NV using the classical analytical solution of beam theory and verified the method using vibration power flow analysis. Applying this analysis to a simple subframe model, we suggested a method of reducing or cutting off vibration to the main body. Future task for FOA for NV are:

- 1) Adoption of Timoshenko's beam theory and development of a useful joint database for greater accuracy.
- 2) Consideration of more complex but real boundary conditions and real outer forces using component synthesis techniques.
- 3) Development of verification methods using detailed mesh FEM models for vibration reduction.

REFERENCES

1. J. W. S. Rayleigh, "Theory of Sound, " 2nd ed., Vol. 1, Dover Publ., New York, 1945
2. D. U. Noiseux, "Measurement of Power Flow in Uniform Beams and Plates," JASA, Vol. 1 Num. 1, (1970), pp. 238-247
3. G. Pavic, "Measurement of Structure Borne Wave Intensity, Part 1: Formulation of the Methods," Journal of Sound and Vibration, 49(2), (1976), pp. 221-230
4. Y. Tsurumi, et al. "First Order Analysis for Automotive Body Structure Design – part 2: Joint Analysis Considering Nonlinear Behavior," SAE Paper, 2004-01-1659 (2004)

CONTACT

The corresponding author of this paper is Toshiaki Nakagawa. He is now working at Toyota Central R&D Labs Inc. His e-mail address is tn@ket.tytlabs.co.jp